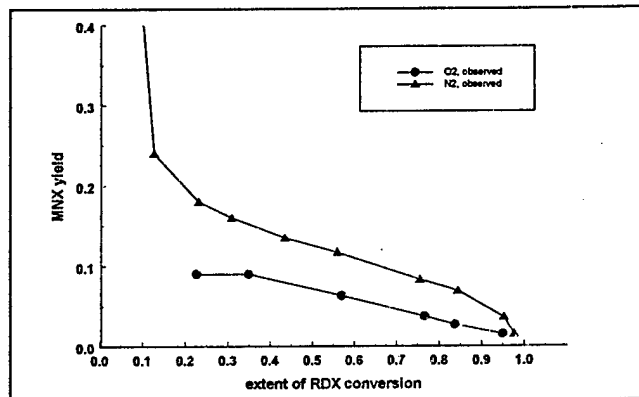




Verification of RDX Photolysis Mechanism

Gary R. Peyton, Mary H. LeFaivre, and Stephen W. Maloney



Nitro-aromatics 2,4,6-trinitrotoluene (TNT) and hexahydro-1,3,5-trinitro-triazine (RDX) are the major constituents of wastewaters discharged from munitions load, assembly, and pack operations at Department of Defense (DOD) facilities. TNT and RDX enter wastestreams during munitions loading and demilitarization. This study focused on a treatment method for RDX.

Prior work has shown that simple photolysis using ultraviolet light (UV) is sufficient to convert RDX in contaminated water to small non-nitrated organic by-products such as formaldehyde and formic acid, as well as the inorganic ions nitrate and nitrite. This implies that UV photolysis might provide a satisfactory and economical treatment system for RDX in water. Although considerable work has been reported in the literature on RDX thermolysis and photolysis pathways, a completely satisfactory mechanism for RDX degradation has not been proposed. Prior work has indicated that a recently elucidated reductive pathway may be

important in the degradation of RDX during photolysis.

The objectives of this project were to postulate a mechanism for RDX photolysis based on information from the literature and data obtained during this study, develop the corresponding kinetic model, and compare projections of that model with results from laboratory photolysis and thermolysis experiments. The results would verify the appropriateness of the model, elucidating the primary mechanistic steps in RDX photolysis and determining whether the reductive pathway contributes significantly to RDX degradation.

A mechanistic model was developed that included all of the reasonable suggestions from the literature. The modeling results indicated that, of the possible pathways given in the literature, the primary photolysis pathway to the nitroso derivative in aqueous solution was removal of an NO₂ group by breaking the N-N bond.

19991227 049

The contents of this report are not to be used for advertising, publication, or promotional purposes. Citation of trade names does not constitute an official endorsement or approval of the use of such commercial products. The findings of this report are not to be construed as an official Department of the Army position, unless so designated by other authorized documents.

DESTROY THIS REPORT WHEN IT IS NO LONGER NEEDED

DO NOT RETURN IT TO THE ORIGINATOR



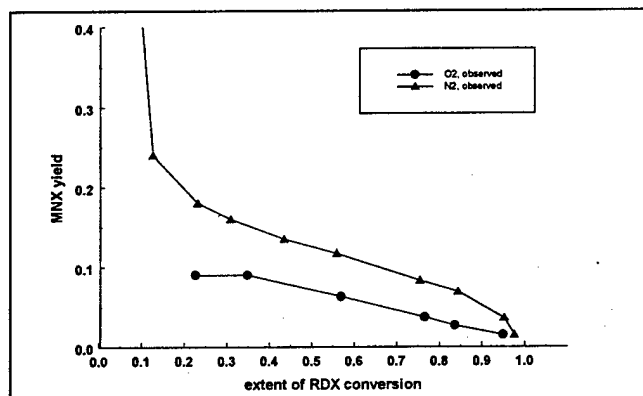
US Army Corps
of Engineers

Engineer Research and
Development Center

CERL Technical Report 99/93
November 1999

Verification of RDX Photolysis Mechanism

Gary R. Peyton, Mary H. LeFaivre, and Stephen W. Maloney



Nitro-aromatics 2,4,6-trinitrotoluene (TNT) and hexahydro-1,3,5-trinitro-triazine (RDX) are the major constituents of wastewaters discharged from munitions load, assembly, and pack operations at Department of Defense (DOD) facilities. TNT and RDX enter wastestreams during munitions loading and demilitarization. This study focused on a treatment method for RDX.

Prior work has shown that simple photolysis using ultraviolet light (UV) is sufficient to convert RDX in contaminated water to small non-nitrated organic by-products such as formaldehyde and formic acid, as well as the inorganic ions nitrate and nitrite. This implies that UV photolysis might provide a satisfactory and economical treatment system for RDX in water. Although considerable work has been reported in the literature on RDX thermolysis and photolysis pathways, a completely satisfactory mechanism for RDX degradation has not been proposed. Prior work has indicated that a recently elucidated reductive pathway may be

important in the degradation of RDX during photolysis.

The objectives of this project were to postulate a mechanism for RDX photolysis based on information from the literature and data obtained during this study, develop the corresponding kinetic model, and compare projections of that model with results from laboratory photolysis and thermolysis experiments. The results would verify the appropriateness of the model, elucidating the primary mechanistic steps in RDX photolysis and determining whether the reductive pathway contributes significantly to RDX degradation.

A mechanistic model was developed that included all of the reasonable suggestions from the literature. The modeling results indicated that, of the possible pathways given in the literature, the primary photolysis pathway to the nitroso derivative in aqueous solution was removal of an NO_2 group by breaking the N-N bond.

Foreword

This study was conducted for Industrial Operations Command (IOC) under 40161102B25 Environmental Research, Corps of Engineers, Work Unit No. J99, "Mechanisms of Rapid Transformation Between Oxidizing & Reducing Radicals." The IOC technical monitor was Chris Vercautren, AMSIO-EQC.

The work was performed by the Environmental Processes Branch (CN-E) of the Installations Division (CN), Construction Engineering Research Laboratory (CERL). The CERL Principal Investigator was Stephen W. Maloney. Gary R. Peyton and Mary H. LeFavre are with the Watershed Science Section of the Illinois State Water Survey. Ilker Adiguzel is Chief, CN-E, and Dr. John Bandy is Chief, CN. The technical editor was Linda L. Wheatley, Information Technology Laboratory.

The Director of CERL is Dr. Michael J. O'Connor.

Contents

Foreword	2
1 Introduction	7
Background.....	7
Objectives.....	7
Approach.....	8
2 Background Literature	9
Overview and Prior Work in This Laboratory.....	9
Nitramine and Nitrosamine Photolysis/Thermolysis Literature.....	10
Organic Photochemistry Literature.....	16
Reactions of Aminyl Radicals.....	21
Participation of NO and NO ₂	22
3 Mechanism and Kinetics	23
Formulation of the Postulated Mechanism of RDX Photolysis.....	23
Development of the Kinetic Model.....	29
<i>Defining the System To Be Modeled</i>	29
<i>Derivation of the Rate Equations</i>	30
<i>Simplification of the Rate Equation Set To Produce Analytical Equations</i>	32
<i>Numerical Integration of the Rate Equations</i>	32
4 Experimental Methods	34
Materials and Apparatus.....	34
<i>Photochemical Reactor Systems</i>	34
<i>Chemicals, Reagents, and Standards</i>	35
Experimental Methods and Procedures.....	35
<i>Analytical Methods</i>	35
<i>Experiments Using Ordnance Compounds – Photolysis</i>	37
5 Results and Discussion	38
Product Yield Diagrams.....	38
<i>Description</i>	38
<i>MNX Yield Diagrams</i>	39
<i>By-Product Yield Diagrams – Formaldehyde</i>	40
<i>Importance of Nitrous Acid Reactions in the Formation of MNX During RDX Photolysis</i>	42

<i>Inorganic Nitrogen Compound Formation During RDX Photolysis</i>	43
Investigations of the MUX Reaction Channel	45
Kinetic Modeling of RDX Photolysis.....	47
<i>Solution of Kinetic Equations</i>	47
<i>Numerical Integration of the Rate Equations and Fitting of Rate Constants</i>	48
<i>Results of Data Fitting</i>	49
6 Conclusions	52
References	53
CERL Distribution	56

List of Figures and Table

Figures

1	RDX and photolysis by-products	10
2	Photolysis of N-nitrosopiperidine	17
3	Photolysis of nitramines	18
4	Pathways of RDX photolytic degradation	24
5	Mechanistic crossovers between nitroso and unsaturated by-products.....	28
6	Effect of 0.5% impurity in chromatogram peak on calculated product yield	39
7	Yield of MNX under oxygenated and deoxygenated (N ₂ sparged) conditions.....	40
8	Formaldehyde yield under oxygenated and deoxygenated conditions	41
9	MNX yield as a function of pH	43
10	Inorganic nitrogen yields under oxygenated conditions.....	44
11	Inorganic nitrogen yields under deoxygenated conditions	44
12	Hydrolysis rate of MUX	46
13	Comparison of model predictions to actual results for oxygenated (O ₂) and deoxygenated (N ₂) conditions	50

Table

1	Equations and rate constants used in the kinetic modeling of RDX photolysis.....	31
---	--	----

1 Introduction

Background

Nitro-aromatics 2,4,6-trinitrotoluene (TNT) and hexahydro-1,3,5-trinitro-triazine (RDX) are the major constituents of wastewaters discharged from munitions load, assembly, and pack operations at current and former Department of Defense (DOD) facilities. TNT and RDX enter wastestreams during munitions loading and demilitarization. Wastewater contaminated with TNT and RDX is referred to as pinkwater, due to its characteristic color. This study focused on a treatment method for RDX.

Prior work has shown that simple photolysis using ultraviolet (UV) light is sufficient to convert RDX in contaminated water to small non-nitrated organic by-products such as formaldehyde and formic acid, as well as the inorganic ions nitrate and nitrite. This implies that UV photolysis might provide a satisfactory and economical treatment system for RDX in water. Although considerable work has been reported on RDX thermolysis and photolysis pathways, a completely satisfactory mechanism for RDX degradation has not been proposed. Recent information has concerned a reductive pathway that may participate in RDX degradation. It is desirable not only to determine whether this pathway is important, but also to clarify the paths by which RDX photodegrades, in order to predict problem by-products and design better treatment systems.

Objectives

The objectives of this project were to:

1. postulate a mechanism for RDX photolysis based on information from the literature and data obtained during this study
2. develop the corresponding kinetic model
3. compare projections of that model with results from laboratory photolysis experiments for the purpose of:

- a. verifying the appropriateness of the model
- b. elucidating the primary mechanistic steps in RDX photolysis
- c. determining whether the reductive pathway contributes significantly to RDX degradation.

Approach

The approach used in this investigation was to:

1. review existing literature to identify all possible candidate reactions that might participate in the pathway
2. construct a mechanistic (pathway) model that includes all candidate reactions
3. eliminate unimportant reactions on the basis of experimental evidence or calculations that show a particular pathway to be unimportant
4. derive the differential rate equations from the reduced mechanism
5. solve these kinetic equations either analytically or numerically while further eliminating unimportant terms
6. identify existing rate constants
7. measure new rate constants if necessary, or estimate their values from literature values for similar rate constants for use in the rate equations
8. use inestimable rate constants as adjustable parameters in fitting the predictions of the kinetic equations to existing and newly acquired experimental data.

Steps 3–8 were used iteratively with acquisition of new data in the laboratory to arrive at a mechanism that satisfactorily described the photolytic degradation of RDX in water.

2 Background Literature

Overview and Prior Work in This Laboratory

Prior work by Peyton et al. (1992), has shown that simple photolysis using UV light is sufficient to rapidly convert RDX in contaminated water to the by-products formaldehyde, formic acid, nitrate, and nitrite. This suggests that photolysis would be an appropriate water treatment process for RDX removal. It is thus desirable to understand how photolysis occurs and what by-products are formed.

Although considerable work has been reported in the literature on RDX thermolysis and photolysis, a completely satisfactory mechanism for RDX degradation has not been proposed. Most researchers have favored the scission (breaking) of the nitrogen-nitrogen (N-N) bond to free nitrogen dioxide (NO_2) as the first step in both thermolysis and photolysis, but as will be shown later in this chapter, published data conflicts with respect to support of that hypothesis. Furthermore, although many investigators have reported the nitroso derivative of RDX (compound MNX in Figure 1) as a major product from both thermolysis and photolysis of RDX, a satisfactory explanation of the mechanism of formation of the nitroso derivative has not been given. Several groups have reported the appearance of the dinitroso-derivative (DNX), and at least one group found the trinitroso-compound (TNX) as well. On the other hand, other researchers have reported identifying the unsaturated compound corresponding to loss of nitrous acid (HNO_2) from RDX (compound MUX in Figure 1), while failing to find the nitroso compounds, leaving the question of the pathways for RDX thermolysis/photolysis unresolved in the literature.

Recently, Peyton et al. (1995), reported the existence of a reductive pathway that was operative even in highly oxidizing systems during the treatment of 2,4-dinitrotoluene (DNT) using hydroxyl radical processes (advanced oxidation processes or AOPs). A mechanism involving reduction to the nitroso compound then to the amino derivative was proposed on the basis of earlier work by Asmus, Mockel, and Henglein (1973) on the radiation chemistry of nitrobenzene. It is reasonable to assume that such a mechanism might be operative in the RDX system as well, which could explain the formation of compounds MNX, DNX, and

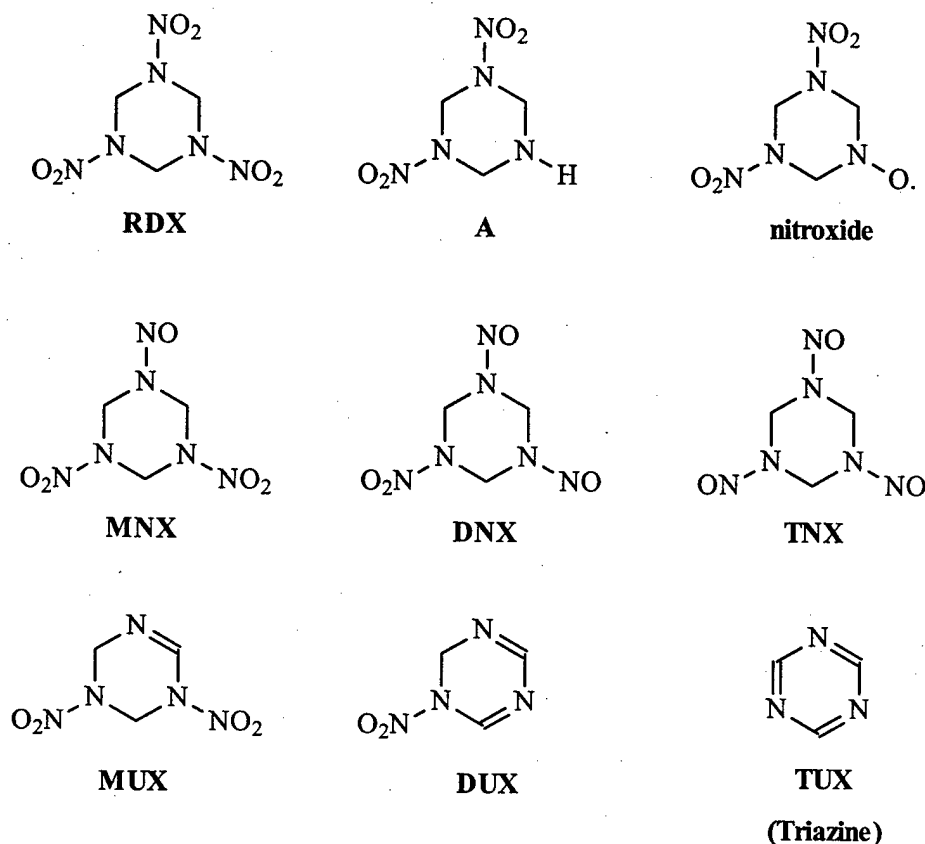


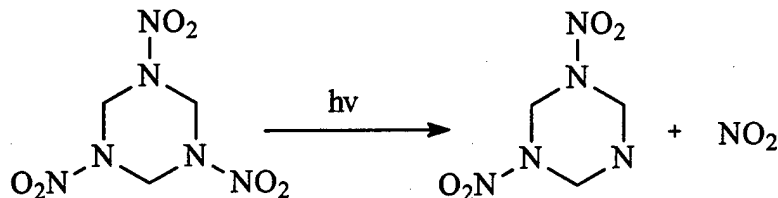
Figure 1. RDX and photolysis by-products.

TNX. This pathway was therefore included among those considered in this study, along with the published reactions discussed in the following sections.

Nitramine and Nitrosamine Photolysis/Thermolysis Literature

Although considerable work has been carried out on the photolysis and thermolysis of RDX in the solid, liquid, and solution phases, there is little agreement in the RDX literature about the reaction pathways during RDX photolysis. Furthermore, results obtained in the solid or gas phase must be used with caution when applying them to the interpretation of solution-phase data. This is due to two factors: (1) in the solid phase, the proximity of other RDX molecules increases the likelihood of interaction with another RDX molecule, and (2) in the gas phase, it can be difficult for intermediate species to rid themselves of excess energy, which can cause decompositions that may not occur in the liquid phase.

A commonly postulated first step in RDX photolysis and thermolysis is scission of the N-N bond, forming NO_2 (a radical, i.e., a very reactive species having an unpaired electron) and an aminyl radical (the remainder of the RDX molecule):



One paper that has been often cited as providing evidence of that reaction is that of Flournoy (1962), who pyrolysed (subjected to high temperatures) dimethylnitramine in the gas phase, determined that the principal product was dimethyl nitrosamine (80 percent yield), and determined an activation energy of 53 ± 5 kilocalorie (kcal)/mole from the temperature dependence of the product appearance rate. The N- NO_2 bond energy in dimethylnitramine had previously been determined to be 55 kcal/mole. On the basis of this agreement, the first-order behavior of the reaction kinetics, and the high yield of a single product, Flournoy proposed a mechanism employing N-N bond scission as the first step.

To test this hypothesis, Suryanarayanan and Bulusu (1972) carried out the photolysis of a mixture of ^{15}N -labeled and unlabeled dimethylnitramine in the solid phase. They interpreted the lack of isotope scrambling in the remaining nitramine as evidence that fission of the N-N bond was not the primary step in RDX photolysis, since some recombination of labeled NO_2 with unlabeled aminyl radical (and vice versa) might be expected due to the diffusional confinement within the solid. These authors instead proposed direct scission of the nitrogen-oxygen (N-O) bond of the nitro group to yield the nitroso group. It is interesting to note, within the context of these results, that the energies of the N-O bonds in N_2O , HONCH_3 , and NO_2 are 40, 50, and 73 kcal/mole (Dean 1987), which are similar to the measured activation energy determined by Flournoy, considering the differences in the parent molecules.

Hoffsommer and Glover (1985) investigated the thermolysis of RDX at 180°C in benzene, deuterated benzene, and as a melt, carried out in evacuated and sealed capillary tubes. They observed the production of the mono-, di-, and trinitroso RDX derivatives (MNX, DNX, and TNX) in high yield, still achieving 75 percent of mass balance with those three products at the 50 percent RDX decomposition point. Products were identified by comparing gas chromatographic (GC) retention times with those of authentic standards synthesized by accepted methods. The gas chromatography/mass spectrometry (GC/MS) spectra of these methods were said to be consistent with the expected product (unfortunately, the spectra

were not published). The authors reported that prolonged thermolysis of the mixture led to an apparent "equilibrium mixture" of nitroso derivatives, and stated that a similar equilibrium behavior was observed during the synthesis of some nitroso derivatives.

Hoffsommer and Glover (1985) also observed a mild solvent kinetic isotope effect of 1.6 on the RDX decomposition rates, which they interpreted as implicating the solvent hydrogen atoms in an interaction with the nitro/nitroso oxygen atoms. They proposed sequential degradation of the nitroso compounds $\text{RDX} \rightarrow \text{MNX} \rightarrow \text{DNX} \rightarrow \text{TNX}$ (Figure 1). They also speculated about a mechanism involving a number of previously proposed processes, but did not provide further supporting evidence. One of the most important contributions of this paper was to provide a simple means for other investigators to prepare retention time standards for the MNX, DNX, and TNX derivatives. This method was used in the present project to identify the MNX, DNX, and TNX peaks in high performance liquid chromatography (HPLC) chromatograms.

Botcher and Wight (1994) performed laser pyrolysis on a ^{15}N -labeled and unlabeled RDX mixture at 77 °K and observed Fourier transform infrared (FTIR) spectra of the frozen products. Scrambled labels in the resultant nitrogen tetroxide (N_2O_4) and a yield of 1.9 RDX molecules decomposed for every N_2O_4 molecule detected was interpreted to mean that one NO_2 came from each decomposed RDX. The authors concluded that N-N bond-breaking to form NO_2 was the first step in RDX thermal decomposition and provided direct evidence for the presence and possible involvement of N_2O_4 in the decomposition.

Oxley et al. (1992) performed thermolysis at 200-300 °C in hydrocarbon solvents, using different ^{15}N singly- and doubly-labeled nitramines. They found that the corresponding nitrosamines were the principal or only condensed-phase products. In agreement with Suryanarayana and Bulusu (1972), they found no scrambling of the nitrogen labels in the reactant nitramine (the authors had expected scrambling would occur if NO_2 ejection was the first reaction step, due to recombination of NO_2 and the aminyl radical), but found complete scrambling in the evolved gases and the product nitrosamines, seemingly inconsistent with NO_2 loss.

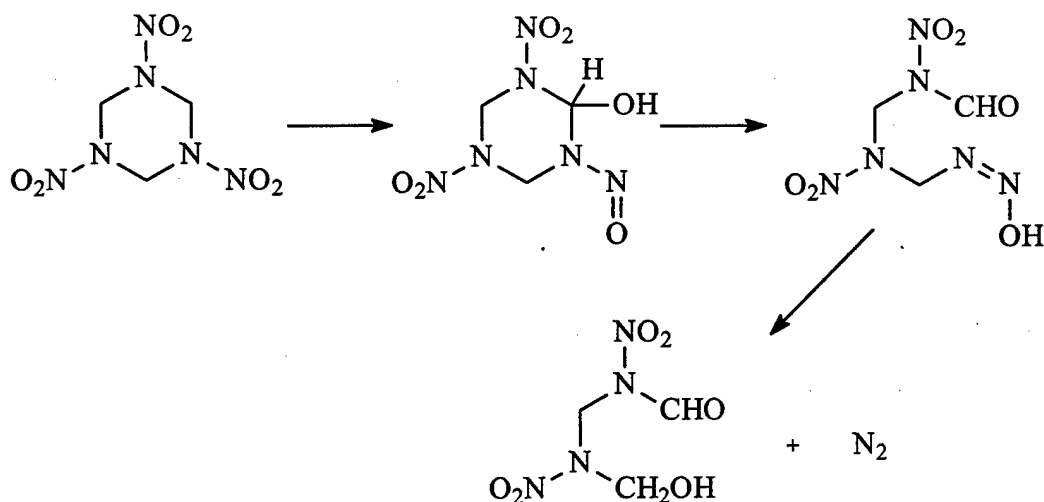
Use of deuterium-labeled dimethylnitramine gave a kinetic isotope effect of 1.57 (in agreement with other workers), indicating involvement of the H-atom adjacent to the N-nitroso group. Of the two possible reactions considered, migration of an O-atom from the NO_2 group to insert in an adjacent C-H bond, or HNO_2 elimination, only the latter explained the isotope scrambling in the nitrogen-containing gases; furthermore, it also explained the absence of carbon oxides in a

similar experiment using diisopropylnitramine. Thus, the authors proposed a mechanism consisting of both N-N bond scission and HNO_2 elimination, but conceded that not all features of their data were explained. The proposed mechanism included dissociation of the N-N bond of the nitramine to give NO_2 and the corresponding aminyl radical from RDX, followed by transformation of the NO_2 into NO (nitric oxide, another radical) by an unspecified mechanism, to give the nitrosamine by recombination of NO with the aminyl radical. The secondary pathway (nitrosamines were the major products in all cases) was postulated to begin with elimination of HNO_2 to give a carbon-nitrogen double bond, to which re-addition of HNO_2 was proposed to yield a hydroxydiazo intermediate that then decomposed to an alcohol. This sequence is shown for dimethylnitramine, where the arrow between nitrogen and oxygen in dimethylnitramine indicates a coordinate covalent bond.



No methanol or formaldehyde was detected by the investigators, so the mechanism was not supported by the product analysis.

A similar reaction to the above sequence, however, cannot occur for RDX without breaking the ring:



Unfortunately, Oxley et al. offered no discussion of reaction products from experiments performed with N-nitropiperidine, which should behave similarly to

RDX with respect to ring cleavage, and therefore might have helped to prove or disprove the authors' hypothesis.

In a later, more extensive study, Oxley and coworkers (1994) reached the same conclusions as before (i.e., that N-N bond scission was the most important pathway, with HNO_2 elimination also a significant reaction). Of the 13 nitramines (including 9 cyclic nitramines) for which thermal decomposition was investigated, the nitrosamine was the principal product for all except RDX. All nitramines were found to have thermolysis activation energies in the 39-52 kcal/mole range. This investigation found some isotope scrambling in the parent nitramine, in contrast not only to the results of Suryanarayanan and Bulusu (1972), but also in contrast to their own previous results. No solvent deuterium kinetic isotope effect was found, in contrast to the results of Hoffsommer and Glover (1985). Compounds with more than one nitramine group showed evidence of sequential conversion to nitrosamines.

Thermolysis of RDX to about 40 percent conversion showed the appearance of MNX, DNX, and TNX, which disappeared at higher conversion, leaving uncharacterizable products. Maximum yields of MNX from RDX were about 24 percent in acetone solution (at 71 percent RDX decomposition), compared to 5-6 percent in the vapor or as the neat compound. In acetone solution, RDX produced about 1 mole of gaseous compounds per mole of RDX heated (240°C for 10 half-lives), half of which was N_2 . As before, the authors concluded that N-N bond homolysis (radical formation) was the principal initial step, followed by conversion of NO_2 to NO (mechanism still unspecified), which recombines with the aminyl radical formed by N-N bond scission. They also showed additional deuterium kinetic isotope effect data to support the secondary mechanism of HNO_2 elimination.

The literature shows additional evidence for the existence of a product corresponding to the elimination of HNO_2 from RDX in aqueous solution, although formed by a different mechanism. Hoffsommer, Kubose, and Glover (1977) detected a semi-stable product from the aqueous alkaline hydrolysis of RDX, measured the kinetics of its disappearance, and obtained the mass spectrum of the products formed from both proteated and deuterated RDX. They assigned the structure as that arising from the removal of a proton from RDX, followed by elimination of NO_2^- to give a product corresponding to MUX in Figure 1. This unsaturated species is the same compound as would be formed by the elimination of HNO_2 as proposed by Oxley et al. Despite the fact that the hydrolysis product disappeared rather quickly (half life of 40-150 minutes at pH 7.9-7.3), Hoffsommer, Kubose, and Glover found only 1.1 mole of nitrite formed by this process, per mole of RDX decomposed, implying that elimination of a second equivalent of HNO_2 did not occur in "weak" base (0.1 M sodium hydroxide

[NaOH] or approximately pH 13), i.e., that sequential elimination to eventually give DUX and triazine (TUX=triazine in Figure 1) did not occur during their alkaline hydrolysis experiments. This, of course, does not rule out the possibility of DUX formation during photolysis.

Even in strong base (19 M NaOH), only 2.1 mole of NO_2^- was found per mole of RDX decomposed, with the remainder of the nitrogen mass balance essentially closed with 0.7 mole of N_2 , 1.6 moles of NH_3 , and 0.4 mole of N_2O per mole of RDX decomposed (5.9 out of 6.0 moles of nitrogen), obviating the formation of triazine in their system.

Hawari et al. (1996) reported the inadvertant production of the unsaturated compound MUX during extraction of RDX from soils using alkaline isopropanol. Although they reported that the compound could be generated in the laboratory by hydrolysis in alkaline 2-propanol, no details were given. A positive-ion chemical ionization (PCI) mass spectrum was shown for the product in which the base peak was at an m/z value of 176, which corresponds to the P+1 peak for the structure of the unsaturated compound MUX.

Bose, Glaze, and Maddox have reported on the results of RDX photolysis in aqueous solution. These authors assigned the NCI (negative-ion chemical ionization) mass spectrum of the primary product to the mono-unsaturated RDX (MUX), but did not find the nitroso derivatives. This assignment, like that of Hawari, must be considered tentative, since (1) the NCI spectra of Bose et al. can not be compared with the EI (electron impact) spectra of Hoffsommer et al. or Hawari. et al., (2) no parent ion (P+M) was observed in the NCI spectrum, (3) no authentic standard compound was available, and (4) no other evidence was given for the assignment. Of the three tentative identifications, those of Hoffsommer et al. and Hawari et al. have the additional evidence that the compound was generated by basic hydrolysis from RDX.

W.H. Glaze, personal communication, 1997. Manuscript submitted to Water Research for publication.

Organic Photochemistry Literature

A review of recent organic photochemistry literature revealed several papers that have not been mentioned in past interpretations of RDX photolysis/pyrolysis data. An extensive series of studies summarized in Chow (1973) and Chow et al. (1979) on the photolysis of nitrosamines and two papers on the photolysis of nitroamines yielded the mechanistic information summarized in Figures 2 and 3, respectively.

Chow found that the behavior of N-nitrosamines such as N-nitrosopiperidine (I in Figure 2) under photolysis was the same whether the $\pi \rightarrow \pi^*$ (340 nm) or $n \rightarrow \pi^*$ (230-240 nm) transition was excited, breaking the N-N bond to form an aminyl radical (II in Figure 2) and nitric oxide (NO). In the presence of acid (0.01 N or stronger), the aminyl radical was rapidly converted to the protonated form, the aminium radical (III in Figure 2). In acidic aqueous solution, this radical is said to be attacked by the counter radical nitric oxide, perhaps forming the intermediate species nitroxyl (NOH) by hydrogen abstraction, and leaving an unsaturated ring compound (IV). Thus, this mechanism produces the same unsaturated compound as does the earlier described HNO_2 elimination but produces nitroxyl rather than HNO_2 .

It is easily shown that application of this mechanism to RDX would produce the same unsaturated compound that was reported by Kubose and Hoffsommer (1977) to arise by hydrolysis. In their paper, Chow et al. (1979) claimed that the nitroxyl then adds to the double bond to give the aldoxime (V). In methanol the aminyl radical was reported to abstract a hydrogen atom from the solvent methanol to yield piperidine and a hydroxymethyl radical (center pathway, Figure 2). The observance of formylpiperidine as a product and the high quantum yield ($\phi = 4-5$) of nitroso compound disappearance appear to be consistent with intermediate generation of a hydroxymethyl radical, which may attack parent nitrosamine, although no specific mechanism was suggested. When an olefin such as cyclohexene was present in acidic solution, addition to the double bond yielded the compound V. In the absence of acid, however, no addition to olefins was observed, and product mass balance was incomplete. Any unreacted nitroxyl radical would dimerize to hyponitrous acid ($\text{H}_2\text{N}_2\text{O}_2$), which is a known reductant that, in the absence of reaction with other species, decomposes to N_2O (Hughes 1968).

Chow et al. (1979) reported that photolysis of the corresponding nitramines under similar conditions also produced the aminyl radical from N-N bond scission, along with NO_2 (Figure 3). In neutral methanol, the corresponding amine pi-

Organic Photochemistry Literature

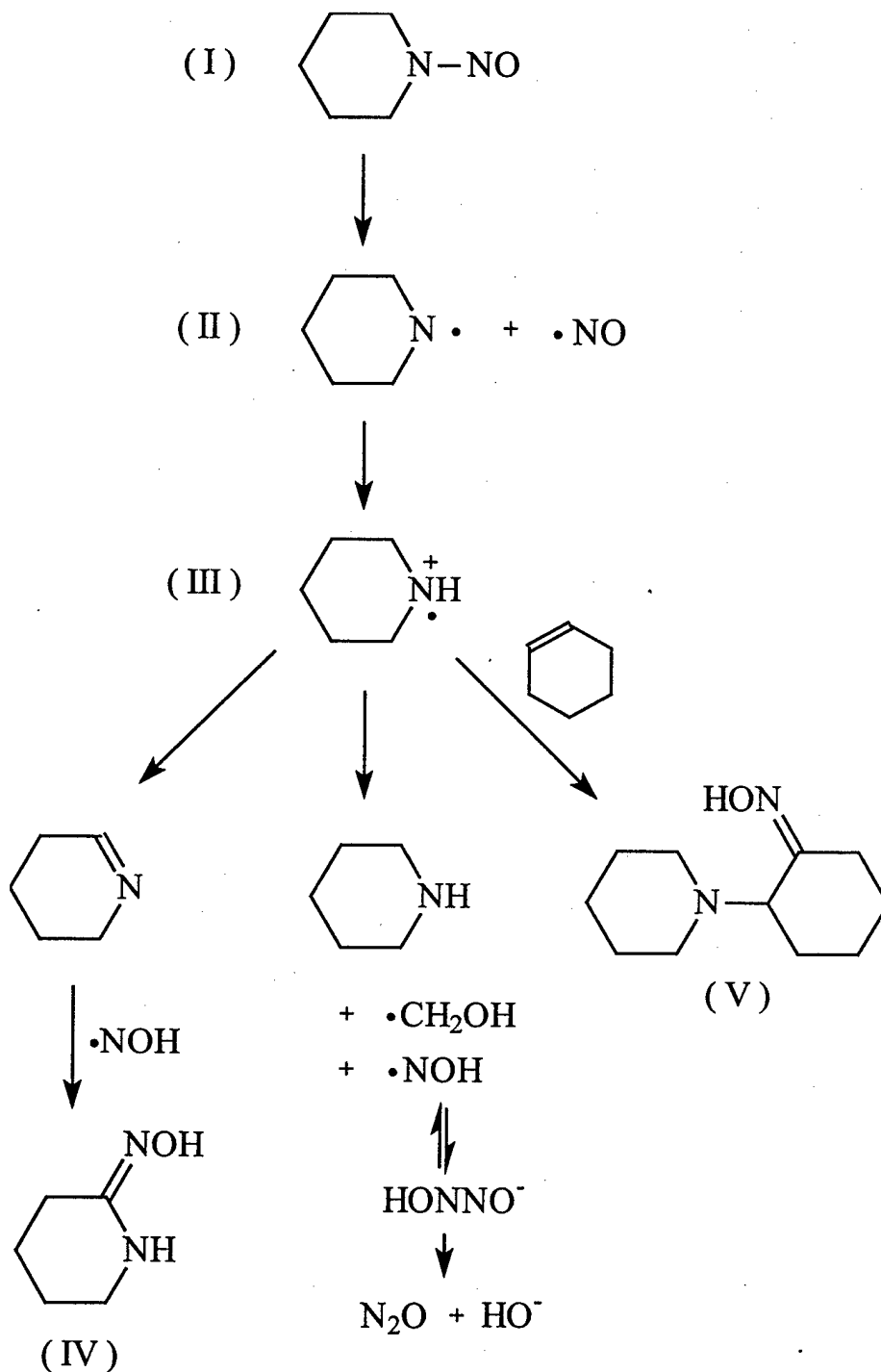
A review of recent organic photochemistry literature revealed several papers that have not been mentioned in past interpretations of RDX photolysis/pyrolysis data. An extensive series of studies summarized in Chow (1973) and Chow et al. (1979) on the photolysis of nitrosamines and two papers on the photolysis of nitroamines yielded the mechanistic information summarized in Figures 2 and 3, respectively.

Chow found that the behavior of N-nitrosamines such as N-nitrosopiperidine (I in Figure 2) under photolysis was the same whether the $\pi \rightarrow \pi^*$ (340 nm) or $n \rightarrow \pi^*$ (230-240 nm) transition was excited, breaking the N-N bond to form an aminyl radical (II in Figure 2) and nitric oxide (NO). In the presence of acid (0.01 N or stronger), the aminyl radical was rapidly converted to the protonated form, the aminium radical (III in Figure 2). In acidic aqueous solution, this radical is said to be attacked by the counter radical nitric oxide, perhaps forming the intermediate species nitroxyl (NOH) by hydrogen abstraction, and leaving an unsaturated ring compound (IV). Thus, this mechanism produces the same unsaturated compound as does the earlier described HNO_2 elimination but produces nitroxyl rather than HNO_2 .

It is easily shown that application of this mechanism to RDX would produce the same unsaturated compound that was reported by Kubose and Hoffsommer (1977) to arise by hydrolysis. In their paper, Chow et al. (1979) claimed that the nitroxyl then adds to the double bond to give the aldoxime (V). In methanol the aminyl radical was reported to abstract a hydrogen atom from the solvent methanol to yield piperidine and a hydroxymethyl radical (center pathway, Figure 2). The observance of formylpiperidine as a product and the high quantum yield ($\phi = 4-5$) of nitroso compound disappearance appear to be consistent with intermediate generation of a hydroxymethyl radical, which may attack parent nitrosamine, although no specific mechanism was suggested. When an olefin such as cyclohexene was present in acidic solution, addition to the double bond yielded the compound V. In the absence of acid, however, no addition to olefins was observed, and product mass balance was incomplete. Any unreacted nitroxyl radical would dimerize to hyponitrous acid ($\text{H}_2\text{N}_2\text{O}_2$), which is a known reductant that, in the absence of reaction with other species, decomposes to N_2O (Hughes 1968).

Chow et al. (1979) reported that photolysis of the corresponding nitramines under similar conditions also produced the aminyl radical from N-N bond scission, along with NO_2 (Figure 3). In neutral methanol, the corresponding amine

piperidine was obtained in 13 percent yield, along with a smaller quantity (7 percent) of formyl piperidine (VI), but product mass balance was again poor. In hexane, 38 percent piperidine was found, along with 33 percent of the corresponding nitroso compound. As is the case of photolysis of nitroso compounds, no



(Reprinted with permission from Chow 1973; copyright 1973 American Chemical Society.)

Figure 2. Photolysis of N-nitrosopiperidine.

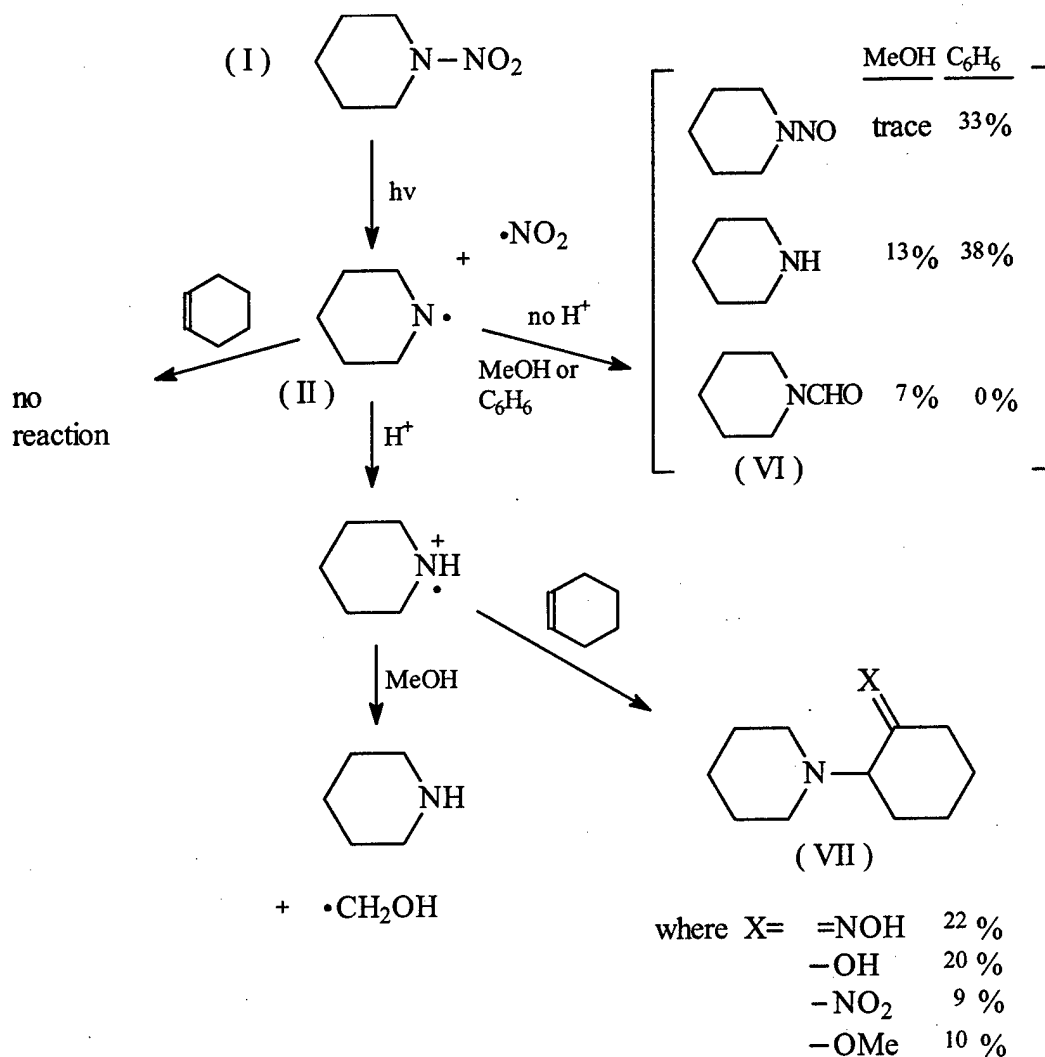


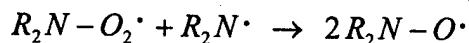
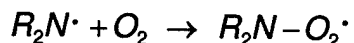
Figure 3. Photolysis of nitramines.

addition to cyclohexene occurred in the absence of acid. In the presence of acid but no cyclohexene, piperidine was obtained, while with cyclohexene present, 73 percent product mass balance was obtained among just the addition compounds (VII). The multiplicity of addition products containing various X groups was consistent with radical addition to the double bond of the alkene as the first step in the reaction. In neutral methanol solution, the quantum yield of N-nitropiperidine (NNP) disappearance was about 5, while in acidic methanol, the quantum yield was 7 to 8, indicating a chain reaction and implying the participation of the hydroxymethyl radical. In acidic methanol, sparging (sprinkling) with oxygen did not reduce the quantum yield of NNP destruction. Unfortunately, no results were reported to indicate that a corresponding experiment might have been carried out in neutral methanol. The intermediacy of the aminyl radical was demonstrated by showing that the same intermediate was reached by

photolysis of N-chloropiperidine, a previously known reaction. Chow et al. (1979) proposed the mechanism shown in Figure 3 to explain their experimental results.

Unfortunately for this photolysis study, the investigations of Chow et al. (1979) focused primarily on the aminium radicals, which were of more interest to those investigators because of their reactivity and synthetic utility. They did not study the neutral aminyl radicals that are the products of nitramine and nitrosamine photolysis in neutral solution, such as are being studied here. In light of the Chow et al. results, it appears significant that Kubose and Hoffsommer (1977) found the production of nitrosamine in acidic but not neutral or basic solution. However, another possible explanation for this result will be discussed in a later section on NO and NO₂ participation. Despite the high values reported for the quantum yields, Chow (1973) stated that the nitramines were photochemically "unreactive" in neutral solution. He later (Ho and Chow 1982) qualified that statement as nitramines being "apparently" unreactive, due to recombination of the aminyl and nitrogen dioxide radicals to regenerate the starting nitramine. This statement was based on a report by Geiger and Huber (1981) that photolysis at 363.5 nm ($n \rightarrow \pi^*$) of gas-phase dimethylnitramine produced dimethylnitramyl radical and NO₂, which recombined with 100 percent efficiency to give starting material. Chow ascribed the greater reactivity of the aminium radical to the fact that it does not recombine with NO₂ as rapidly as does aminyl radical.

The general results of Chow et al. (1979) were supported by those of Wagner, Ruel, and Luszyk (1996), who also found that the lifetime of the aminium radicals was longer in 2:1 methanol:water than in acetonitrile. This point might at first seem to conflict with Chow's mechanism, but that conflict might be accounted for by the fact that the NO₂ concentration could be depleted by reaction with methanol and water, leaving less NO₂ to back-react with aminium radical. Wagner, Ruel, and Luszyk (1996) also found that the spectra and lifetimes of the radicals formed were unaffected by the presence of oxygen, implying no nitroxide production by:



since the spectrum of the nitroxide should be detectable and radical lifetimes noticeably shortened by reaction with O_2 . It is more likely that nitroxide would be formed by (Schuchmann and von Sonntag 1997):



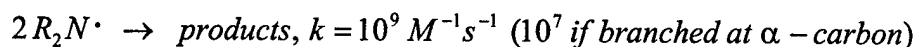
The results of Wagner, Ruel, and Luszyk (1996), appear at first to be in direct conflict with those of Roberts and Ingold (1973), who performed electron spin resonance (ESR) studies that conclusively demonstrated nitroxide formation due to rapid and quantitative reaction of aminyl radicals with oxygen. The nitroxide formed from 2,2,6,6-tetramethylpiperidyl (TMP) radicals was shown to have the same esr spectrum as an authentic sample of the nitroxide. Nitroxides are relatively stable free radicals (i.e., many can be isolated under some conditions) and are used for "spin trapping" in mechanistic studies. These investigators reported that TMP radicals abstracted hydrogen atoms from their hydrocarbon solvents with rate constants ranging from $0.69 M^{-1}s^{-1}$ for toluene to 0.013 for 2,3-dimethylbutane. The reaction of TMP with O_2 was reportedly too fast to measure under their conditions. However, calculation of the fastest rate constant for reaction with O_2 that these investigators could measure gave $k' > 10^4 s^{-1}$, while the slowest rate constant that Wagner could have detected in competition with quenching by the solvent was on the order of $10^6 s^{-1}$. Therefore, these two reports are not in conflict, and it is a reasonable assumption that $10^4 < k' < 10^6$. This value would not necessarily apply to the particular aminyl radical produced from RDX, but gives at least a starting point for estimation of such a value. A more recent review of the chemistry of nitroxides (Aurich 1989) still supports the conclusions of Roberts and Ingold (1973) as do Schuchmann and von Sonntag (1997). However, another paper by von Sonntag and Schuchmann (1997) also raises the possibility of elimination of HO_2 by the nitrogen-centered peroxy radical and a hydrogen atom from an adjacent carbon atom, to yield a carbon-nitrogen double bond. In the case of the aminyl radical formed by loss of NO_2 from RDX, this would lead to the same unsaturated compound (MUX) described above as arising from the elimination of HNO_2 .

In an earlier paper, Bowman, Gillian, and Ingold (1971) reported measured rate constants for bimolecular disappearance of the nitroxide radicals, finding values of 2×10^4 to $7 \times 10^5 M^{-1}s^{-1}$ in going from the nitroxide of dimethyl amine to piperidine. The sterically-hindered diisopropyl amine nitroxide reacted more than three orders of magnitude slower.

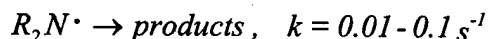
Reactions of Aminyl Radicals

The results cited above suggest that it is reasonable to assume that photolysis of RDX proceeds via N-N bond scission, forming an aminyl radical and NO₂, as suggested by Oxley et al. (1994) and others. This assumption in turn suggests that the characteristics of aminyl and aminium radicals in aqueous solution should be further investigated for clues as to the subsequent degradation steps during RDX photolysis. Compilations of rate constants reported for these radicals are available prior to 1983 in Ingold and Roberts (1983). Although the list of examples is by no means complete, typical values can be summarized as follows.

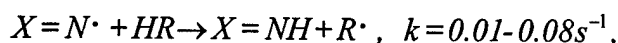
Self-reaction —



Unimolecular decomposition —



Hydrogen abstraction —



In addition to these typical values, a specific value has been reported for the reaction of piperidyl radical with methanol ($3.8 \times 10^4 M^{-1}s^{-1}$).

For the corresponding aminium (positive) radicals, self-reaction was two to four orders of magnitude slower than that of the aminyl (neutral) radicals (due to repulsion of two positive charges), while unimolecular decomposition and hydrogen abstraction reactions were considerably faster ($5-7 \times 10^3$ and $1-4 \times 10^4 M^{-1}s^{-1}$, respectively). Although the term "unimolecular decomposition" was used in the reference, it may be misleading, since the reactions were carried out in solution and the possibility of solvent participation cannot be ignored (see next section). The

bimolecular reaction is thought to proceed by disproportionation,* which was suggested without support by Chow et al. (1979) as the fate of the aminyl radical in neutral solution. This, however, is a reasonable assumption, as many types of free radicals are known to disproportionate in bimolecular reactions.

Participation of NO and NO₂

The role ascribed to NO and NO₂ in the nitramine studies cited above was largely ignored or invoked in unspecified steps to accomplish nitration or justify product distribution. Credibility of this mechanism of nitrosation by nitrogen oxides in aqueous solution was hampered by the belief that hydrolysis of NO₂ in water was too rapid to permit other reactions, and would therefore fail to lead to nitrosation of a substrate to form nitrosamines. Direct nitrosation by nitrous acid, while used preparatively, is too slow to explain the rapid formation of nitrosamines during RDX photolysis (Casado et al. 1984) and takes place at pH much lower than neutral. Important information has, however, been provided by Challis and Kyrtopoulos (1978; 1979), who showed that NO produced nitrosamines from secondary amines only very slowly (half-life of 8 days), but that the introduction of air into the same system resulted in immediate (<1 minute) production of the corresponding nitrosamines. This was shown to be due to the oxidation of nitric oxide to NO₂, followed by formation of N₂O₃ and N₂O₄, which rapidly nitrosated the secondary amines, despite reports that NO₂ quickly disproportionates to nitrate and nitrite in water (average value† of $k=7 \times 10^7 \text{ M}^{-1}\text{s}^{-1}$). These authors presented evidence that nitrosation occurs considerably faster than hydrolysis. Values of the second-order rate constant for reaction of N₂O₃ with 29 primary and secondary amines have been determined by Casado et al. (1983), who found that the rate constants for all 18 saturated amines studied fell in the range 7.5×10^7 - $3.1 \times 10^8 \text{ M}^{-1}\text{s}^{-1}$. This evidence for the survival of the N₂O₃ and N₂O₄ species in aqueous solution long enough to nitrosate secondary amines is key information in the search for a mechanism that would explain the present data, since it makes Chow's proposed mechanism (Figures 2 and 3) even more plausible. The information presented in this chapter supplies several steps that were missing from previously proposed mechanisms and allows the postulation of a comprehensive mechanistic pathway for photolysis of RDX.

* The changing of a substance, usually by simultaneous oxidation and reduction, into two or more dissimilar substances.

† Average value calculated from values tabulated in Neta, Huie, and Ross 1988.

3 Mechanism and Kinetics

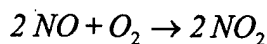
Formulation of the Postulated Mechanism of RDX Photolysis

The primary photochemical step in RDX photolysis is assumed to be N-N bond scission, based on the photochemical work of Chow and coworkers, discussed in Chapter 2. This pathway is supported by the results of Oxley and coworkers, who also postulated this reaction and the loss of HNO_2 as the first steps. However, it is not necessary to assume a parallel primary reaction that produces the unsaturated product MUX, as this product can be reached by other pathways. Similarly, it was assumed by Oxley that MNX is formed primarily by the reaction of aminyl radical with NO, a radical-radical reaction that would be expected to be fast (i.e., large value for the rate constant). However, the initial path from NO_2 to NO was not specified by Oxley, and no satisfactorily direct conversion pathway has been found in the present study. This dilemma is solved in the present mechanism by assuming that nitrosamine production occurs by the nitrosation of the corresponding amine by N_2O_3 and N_2O_4 , as demonstrated by the work of Challis and coworkers, discussed in Chapter 2. This is consistent with the finding of the presence of N_2O_4 by Botcher and Wight (1994) and accounts for N-scrambling in the products as reported by Oxley et al. (1992). Production of NO indeed may occur later by photolysis of the nitroso compound, and some NO may react with aminyl radical at this point, to *regenerate* nitroso compound, but this reaction is not required as a primary pathway to nitroso compound.

The proposed pathway network for RDX photolysis in water is detailed in Figure 4. Capital letters given in parentheses are the symbols used to represent those compounds in the equations used for the kinetic analysis, which follow. Two sets of symbols are used because the 3-letter acronyms (e.g., MNX) are more descriptive in the text, but single-letter shorthand symbols are more suitable as subscripts in equations.

The proposed primary photochemical process is N-N bond scission to produce a nitrogen-centered aminyl radical R. The primary pathway to nitroso compounds is by hydrogen atom abstraction by the aminyl radical to form the corresponding amine A. This amine is then quickly nitrosated by N_2O_3 and/or N_2O_4 , giving the mononitroso RDX derivative MNX (shorthand symbol M). N_2O_4 (symbol T) is produced by the dimerization of NO_2 (symbol N), which is in competition with the

N_2O_3 . Reaction of NO with oxygen has recently been studied (Awad and Stanbury 1993), and the reaction found to be third order:



with a reaction rate constant of $k_{CR} = 2 \times 10^6 \text{ M}^{-2} \text{ s}^{-1}$.

MNX can also photolyze by losing an NO_2 group (indicated by the arrow labeled with k_p in Figure 4), which can lead to the dinitroso analog of RDX (DNX) through reaction of the radical thus formed with NO, and presumably by reaction of the amine corresponding to MNX with N_2O_3 and N_2O_4 , by analogy with RDX. The analogous set of reactions, applied to DNX leads to TNX. Thus, MNX, DNX, and TNX are all in photo-equilibrium with their respective aminyl radicals, NO and NO_2 , and therefore with each other. This is consistent with the observations of Hoffsommer and Glover (1985) that the nitroso product distribution appeared to reach an equilibrium during both synthesis and thermolysis, and those of Oxley et al. (1994) that nitrosation was sequential. As the parent compound RDX is consumed, the main source of NO_2 disappears, and attrition of NO and NO_2 through competing oxidative and hydrolytic pathways depletes the nitrosating agents N_2O_3 and N_2O_4 , resulting in eventual loss of the nitroso derivatives through the competing non-nitrosating reaction channels for R (i.e., the reactions that lead to MUX in Figure 4).

Aminyl radical R is converted to amine A by H-atom abstraction from a suitable donor (D in Figure 4), the most likely of which is formaldehyde produced in high yield as a byproduct (see Chapter 5). This reaction produces the formyl radical and its hydrate dihydroxymethyl radical, which are both strong reducing radicals, whose fate is discussed below. The reaction rate constant for the reaction of the aminyl radical from piperidine with methanol has been measured (Chow 1973) to be $3.8 \times 10^4 \text{ M}^{-1} \text{ s}^{-1}$. It is expected that reaction with formaldehyde and its hydrated form would be somewhat faster, by comparison of the hydroxyl radical rates of reaction with methanol and formaldehyde. Furthermore, the aminyl radical from RDX is more electron poor than that from piperidine, which should result in an even higher reaction rate for the aminyl radical from RDX. It should be noted that in nonaqueous solvents, the solvent could serve as the H-atom donor D, leading to a higher formation rate of donor radical S.

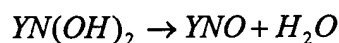
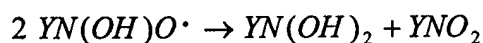
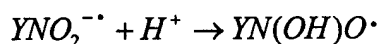
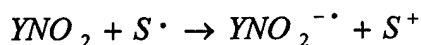
Disproportionation of the aminyl radical is expected to be fast, and would also lead to the formation of A in 50 percent yield based on R, the other half forming unsaturated derivative MUX. This provides one pathway for MUX production

that does not directly involve RDX. This pathway requires relatively high radical concentrations in order to be important, since it is bimolecular in aminyl radical.

A third pathway that was considered for amine formation is electron transfer from nitrite ion to the aminyl radical, followed by protonation. Nitrite is also formed as a reaction by-product in relatively high yield (see Chapter 5 results). No precedent for this reaction was found in the literature, and since it was determined during the modeling phase of the project (discussed on p 29) that this reaction contributed nothing to the modeling results that could not be accomplished through other pathways, it was dropped from consideration during modeling.

Other degradation pathways to aminyl radical, which do not lead to formation of amine A, are available. Reaction with oxygen to form an N-peroxyl radical could lead to either a nitroxide or MUX, depending on whether reaction of the peroxyl radical with another aminyl radical or peroxyl radical was faster than HO₂ elimination from the N-peroxyl radical. Rearrangement of an aminyl radical to a carbon-centered radical (by transfer of an H-atom from the alpha carbon to the nitrogen atom of R) has been invoked to explain the reaction pathways of aliphatic amines with hydroxyl radical. The carbon-centered radical would be expected to add oxygen at almost diffusion-controlled rates, forming a peroxyl radical that would rapidly eliminate HO₂ (see discussion of von Sonntag's work, Chapter 2) to give MUX. Thus, two more pathways that do not directly involve RDX are available for MUX formation.

A second pathway for RDX consumption was investigated, in which reducing donor radical S reacts with the nitro group of RDX, reducing it to the radical anion (Q in Figure 4). This process has been shown (Asmus, Mockel, and Henglein 1973) to result in the reduction of nitrobenzene to nitrosobenzene and was the first step in the reductive treatment of 2,4-dinitrotoluene (DNT) in oxidizing media reported by Peyton et al. (1995). The radical anion protonates, then disproportionates to give back one molecule of the original nitro compound and one molecule of nitroso derivative.



In these equations $YNQ_2^- = Q$ from Figure 4. The intermediate steps shown above are omitted in Figure 4 for simplicity, since they do not affect the rest of the reaction system.

It has recently been shown in this laboratory that RDX can be quantitatively reduced to the nitrosamine by the reducing 1-hydroxyethyl radical with rate constant $1.2 \times 10^7 \text{ M}^{-1} \text{ s}^{-1}$ (Peyton et al., unpublished data). This reaction probably proceeds by a pathway analogous to that shown above for nitrobenzenes, through the intermediate radical anion Q, which disproportionates to give MNX and RDX. For this reason, the reductive pathway through Q to MNX was also considered in this study.

Thus, the mechanism constructed from the sum of known reactions provides two main pathways to MNX: dissociation of the N-N bond and direct reduction of RDX by a reducing radical. It is interesting that this reaction network also provides multiple pathways to the unsaturated compound MUX in addition to the possibility of any "direct" elimination of HNO_2 , which is the pathway that has typically been considered in the RDX thermolysis/photolysis literature to produce the unsaturated compound.

The first stable by-product, MNX, must undergo an additional photolysis reaction in order to produce DNX by the mechanism described. This reaction, which is analogous to the initiation reaction by RDX to produce R, would give a nitrogen-centered triazine radical containing one nitro and one nitroso group. Its production is indicated in Figure 4 as the arrow with the rate constant k_p leading to radical R_2 . It is reasonable to expect that this new aminyl radical also undergoes a system of reactions analogous to those shown in Figure 4, and it follows that those from DNX and TNX would as well. Furthermore, the unsaturated products MUX and DUX (if the latter is formed) would also be expected to photolyze, forming intermediates that contained both nitroso groups and unsaturation. The unsaturated compounds formed in these series of products would also be expected to hydrolyze, by analogy with both less unsaturated (MUX) and more unsaturated imine (containing a " $-\text{N}=\text{CH}-$ " functionality) compounds such as TUX (triazine). Triazine has been reported to hydrolyze rapidly in water, going from 10 percent aqueous solution to nondetectable in 10 min, and forming inorganic salts such as ammonium formate (Smolin and Rapaport 1959). The result of these mechanistic "crossovers" between the nitroso channel and the unsaturated channel is the possibility of nine by-products that incorporate combinations of nitrosation and unsaturation. This situation is represented in Figure 5, where NUX contains one unsaturation and one nitroso group, UUN contains one nitroso group and two unsaturations, and UNN contains two nitroso groups

and one unsaturation. As stated before, since MUX and triazine are hydrolytically unstable, it is reasonable to assume that all compounds to the left of the dashed line in Figure 5 are hydrolytically unstable as well, implying a great number of smaller molecular by-products. The fact that nitrite and formaldehyde quickly appear as by-products during RDX photolysis in aqueous solution (see Chapter 5 results) implies that, beyond a certain point, by-products "unzip" to the final by-products rather easily. The fact that formaldehyde is observed, rather than formic acid, may indicate that triazine is probably not formed, but that result must be qualified somewhat (see Chapter 5 results). Under these conditions, identification of the unstable products for the purpose of verifying a mechanism would be quite difficult.

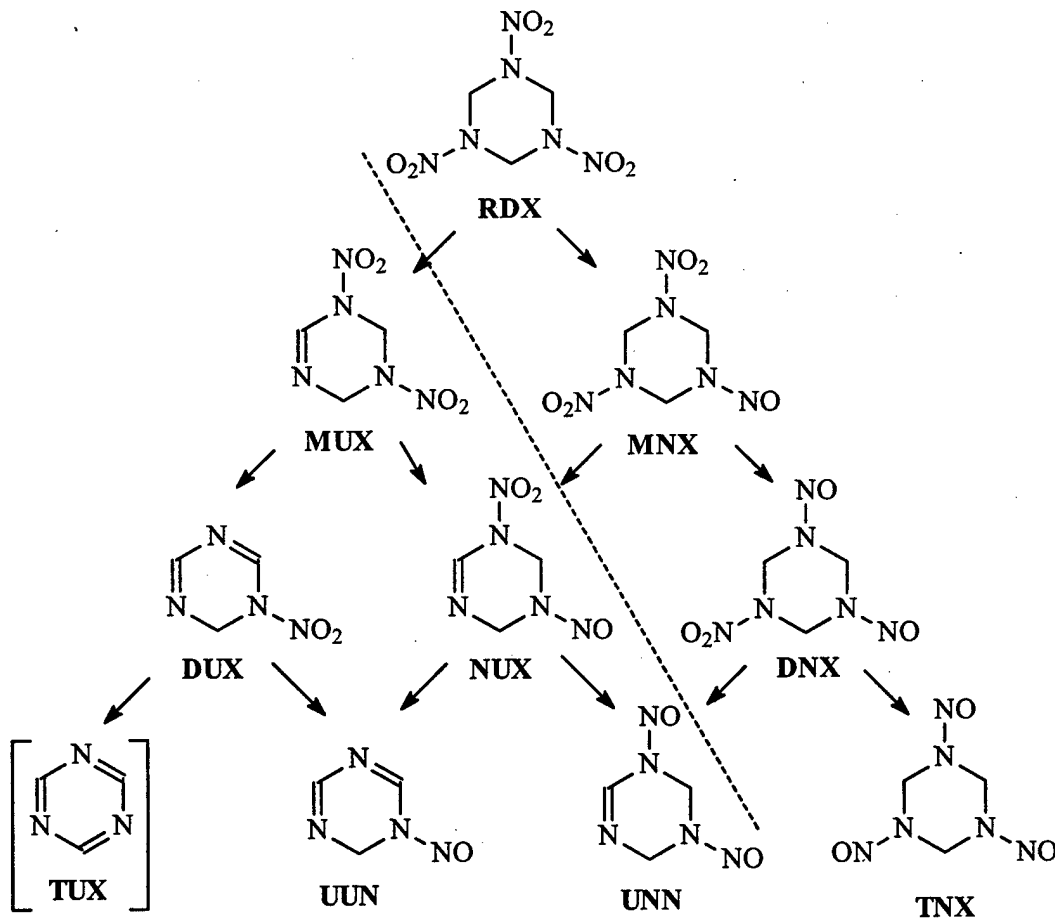


Figure 5. Mechanistic crossovers between nitroso and unsaturated by-products.

Development of the Kinetic Model

Defining the System To Be Modeled

The full degradation path network that describes the formation of the triazine by-products shown in Figure 5, as well as the small intermediate molecules resulting from hydrolysis of those by-products, is not complete at this time, but even if it were, the system would be too large and complicated for kinetic modeling. For this reason, a subsystem of the mechanism must be selected and used to support or refute the general characteristics of the mechanism, before modeling the larger system can be attempted. Even the entire pathway network that is described in Figure 4 is unsuitable for modeling, because no stable products have been identified for the left-hand side of the mechanism (MUX-related pathways). One of the products that was detected was tentatively assigned the structure of MUX (see Chapter 5 results), on the basis of comparison of its hydrolytic lifetime in solution with that from Hoffsommer, Kubose, and Glover (1977), as well as the fact that several other investigators have reported its identification. The reactions proposed to lead to MUX are all known reaction types in the literature. However, except for triazine, no authentic standards are available for the proposed unsaturated products in Figure 5, and without quantitative data on the unsaturated derivatives, it is pointless to try to quantitatively model the left-hand side of the mechanism. In view of the evidence that will be presented for the facile hydrolysis of these intermediates, it is probably sufficient to state (on the basis of prior work on MUX and triazine) that unsaturated triazines are unstable and decompose to small molecules. The accumulation of a high yield of formaldehyde (see Chapter 5 results) supports that conclusion.

The initial kinetic investigation was therefore limited to the portion of the mechanism that involves the formation and destruction of the first observable stable product, MNX, shown in the right-hand side of Figure 4. Not only were the nitroso MNX, DNX, and TNX observed to be quite stable for days under laboratory conditions, but they are also of toxicological importance. In addition, the elusiveness of a satisfactory mechanism in past studies makes it of interest to determine whether the recently discovered pathways involving reducing radicals play a previously unrecognized role in the formation of the nitroso derivatives. Finally, intermediate products involved in the nitroso branch of the degradation network are quantifiable, permitting modeling to support proposed mechanisms and investigate the effect of oxygen on the reaction pathways. Successful modeling of this subsystem could lay the groundwork for the extension of the central mechanism developed for the MNX subsystem to DNX and TNX as well. It can also provide information on the input to the MUX channel of the mechanism, for

use in modeling that channel as more information on products becomes available.

Several steps in the right-hand side (MNX channel) of Figure 4 are postulated from similar types of known reactions for other compounds, but have not yet been observed for the specific reactants shown in Figure 4; therefore, rate constants for these steps have not been measured and reported. This means that modeling the mechanism requires estimating or measuring unknown rate constants and/or using them as variational parameters in a fit of the kinetic equations to experimental data. This modeling must be done with caution since, in models with a large number of fitting parameters, it is often easy to obtain a fit that appears to describe the data, but in reality has no relationship to the actual mechanism.

Derivation of the Rate Equations

The first step in modeling the MNX subsystem was to derive the system of rate equations from the mechanistic model. In the kinetic modeling of the MNX subsystem, only two pathways for RDX destruction were explicitly described: direct photolysis to produce NO_2 and an aminyl radical, and reduction of RDX by the reducing radical S. The fraction of photolyzed RDX that led to aminyl radical was designated f_1 , implying that fraction $1-f_1$ could lead to other pathways that did not involve aminyl radical or MNX (such as elimination of HNO_2 to yield MUX), with f_1 to be used as a parameter. The species central to the reaction network is the aminyl radical R, which can decay by six different pathways (Figure 4), three of which take it out of the subsystem involving MNX (rearrangement, reaction with oxygen, and the half of the disproportionation channel that leads to MUX). Differential rate equations were written for the twelve species included in the original model (RDX, MNX, Q, A=amine, B= NO_2 , C=NO, N= NO_2 , T= N_2O_4 , E= N_2O_3 , D=H-atom donor, S=donor radical, and R=aminyl radical).

Reactions considered and initial values of the rate constants used are shown in Table 1. When seemingly reliable values of the rate constants for a particular reaction were available, those values were used. When all that was available was a rate constant for a similar reaction, a range of values one or two orders of magnitude on either side of the sample rate constant was considered. In cases where no sample value was available, a best guess was made and the sensitivity of the system to that value was tested. Table 1 lists the references cited for values of rate constants or sample rate constants, and/or the method used to arrive at the initial value. Equations were constructed in the usual manner, with a unimolecular reaction contributing a first-order term to the rate equation of all species involved, bimolecular reactions contributing a second-order term, etc.

Table 1. Equations and rate constants used in the kinetic modeling of RDX photolysis.

Reaction	Value	Reference. (notes)
$RDX \xrightarrow{h\nu, k_1} R + NO_2$	$1.3 \times 10^{-3} s^{-1}$	(a)
$RDX + S \xrightarrow{k_{SC}} Q + product$	$1.0 \times 10^6 M^{-1} s^{-1}$	(b)
$R + R \xrightarrow{k_{RR}} A + MUX$	$1.0 \times 10^9 M^{-1} s^{-1}$	(c)
$R + Donor \xrightarrow{k_{RD}} A + S$	$1.0 \times 10^5 M^{-1} s^{-1}$	(d)
$R + O_2 \xrightarrow{k_{RX}} RO_2$	$8.0 \times 10^3 M^{-1} s^{-1}$	(e)
$R \xrightarrow{k_{rt}} carbon\ radical$	$1.0 s^{-1}$	(f)
$R + NO \xrightarrow{k_{CR}} MNX$	$1.0 \times 10^9 M^{-1} s^{-1}$	(c)
$S + O_2 \rightarrow peroxy\ radical$	$2.0 \times 10^9 M^{-1} s^{-1}$	(c)
$A + N_2O_3 \xrightarrow{k_{EA}} MNX + NO_2^-$	$1.0 \times 10^9 M^{-1} s^{-1}$	(g)
$A + N_2O_4 \xrightarrow{k_{AT}} MNX + NO_2^-$	$5.0 \times 10^8 M^{-1} s^{-1}$	(g)
$NO_2 + NO_2 \xrightarrow{k_N} N_2O_4$	$4.5 \times 10^8 M^{-1} s^{-1}$	(h)
$NO + NO_2 \xrightarrow{k_{CN}} N_2O_3$	$1.1 \times 10^9 M^{-1} s^{-1}$	(i)
$2NO_2 + H_2O \xrightarrow{k_h} NO_2^- + NO_3^- + 2H^+$	$7.0 \times 10^7 M^{-1} s^{-1}$	(j)
$2NO + O_2 \xrightarrow{k_{CX}} 2NO_2$	$2.0 \times 10^6 M^{-1} s^{-1}$	(k)
$MNX \xrightarrow{h\nu, k_M} R + NO$	$1.0 \times 10^{-3} s^{-1}$	(l)
$MNX \xrightarrow{h\nu, k_P} R' + NO_2$	$1.5 \times 10^{-3} s^{-1}$	(l)

Notes:

(a) Measured experimentally in this laboratory. (b) Estimated from measured value of $1.0 \times 10^7 M^{-1} s^{-1}$ for RDX + 1-hydroxyethyl radical. (c) Estimated, based on typical aminyl radical-radical reactions. (d) Estimated, based on comparison with $k_{MeOH, piperidyl} = 3.8 \times 10^4 M^{-1} s^{-1}$. (e) Value estimated from literature to be approximately $10^4 < k_{RX} < 10^6 M^{-1} s^{-1}$. Value of 8.0×10^3 arrived at by fitting oxygen dependence data. (f) Value unknown. Present value obtained by fit. (g) Values for similar reaction of 18 amines were found to be in the range 7.5×10^7 to 3.1×10^9 . Listed value obtained by fit. (h) Graetzel et al. 1969. (i) Graetzel, Taniguchi, and Henglein 1970. (j) Average of first three values listed in Neta, Huie, and Ross 1988. (k) Awad and Stanbury 1993. (l) Estimated to be similar to k_r . Listed value obtained by fit.

Simplification of the Rate Equation Set To Produce Analytical Equations

The first attempt to model the MNX subsystem was the simplification of the rate equations, with the goal of obtaining analytical expressions to be used in data analysis. The steady-state approximation was invoked for radicals R, S, C, N, and Q, and for the very reactive species N_2O_4 (T) and N_2O_3 (E). Their rate equations were solved and the resulting expression for each species consecutively substituted into the other equations to eliminate those variables from the remaining equations for RDX (G), MUX (M), and amine (A). Since the amine (A) has not been identified among the products, and no known authentic standard is available, the behavior of A cannot be verified; therefore, no valid estimate of the amine concentration could be made. For the other species, however, estimates of the concentrations can be made, and were used to eliminate insignificant terms from the rate equations. The only place that the amine concentration A appeared in the resulting equations was in the expression for the fraction of nitrogen tetroxide ($N_2O_4 = T$) captured by A:

$$f_{AT} = \frac{k_{TA} A}{k_{TA} A + k_T}$$

This fraction was therefore considered as a parameter.

Similarly, although nitrite data were collected in some experiments, the rate constant k_{RB} for reaction of radical R with nitrite is not known, so f_{RB} , the fraction of R radical reacting with nitrite, cannot be evaluated with certainty. Finally, reaction of C (NO, nitric oxide) with radical R is said to be very fast, but the rate constant for rearrangement of radical R to the carbon-centered radical may also be fast, and neither rate constant is known. Therefore, f_{CR} is also unknown.

Numerical Integration of the Rate Equations

Analytical solution of the rate equations is preferable to numerical integration because, during analytical solution, constants often group in clusters that recur in various equations, indicating that the cluster has special significance, and providing insight into the workings of the mechanism. Often, however, analytical solution is not feasible, or leads to results that cannot be evaluated because of lack of rate constant or concentration data. In these instances, commercial software for the solution of differential equations is used to integrate the set of simultaneous equations. Although this method provides less mechanistic information than an analytical solution, it does provide concentration data from which the amount of reaction going through various channels can be calculated. The

solver must be capable of handling "stiff" differential equations, but most of the solvers currently on the market have that capability. The software Scientist™ by MicroMath® was used in this study.

4 Experimental Methods

Materials and Apparatus

Photochemical Reactor Systems

Small stirred-tank reactor.

A continuously stirred tank reactor (CSTR) that required an initial solution volume of 1 L was used for experiments in which the use of larger solution volumes was desirable. The reactor consisted of a borosilicate resin kettle with a liquid volume of 1.1 L. The lips of the vessel and the accompanying cover were flanged and finely ground for a tight seal. The cover provided four ports through 24/40 standard taper joints. A wooden collar, which had eight evenly spaced holes drilled into it, was placed over the upper side of the flanged lip of the cover and was secured by the use of bolts and wing nuts to a matching wooden collar placed on the lower side of the flanged lip of the kettle. Use of a silicone rubber gasket between the glass flanges, along with the collar system, provided an airtight closure for the kettle.

The center joint of the cover held a stirring gland that accommodated a glass shaft to which a teflon stirring paddle was attached. A Cole Parmer variable-speed lab mixer powered the stir paddle with the stirring rate governed by a Cole Parmer Stir-Pak Solid State Controller. Two of the exterior openings contained the quartz lamp wells for the UV lamps. The remaining opening was fitted with a four-way glass connecting tube which provided three outer joints as access for sampling and the introduction of a gas diffusion tube. One side arm of this connecting tube ended with a 24/40 standard taper outer joint. The major arm of the four-way connector ended in twin angled joints (Ace-Thred, 24/25 joint), each of which was threaded to accommodate a nylon bushing and viton o-ring packing around 1/8-in. polytetrafluoroethylene (PTFE) tubing entering and leaving the reactor.

The UV lamps were Analamp low-pressure mercury lamps (Model # 81-1057-01) purchased from BHK, Inc. The majority of the emission (i.e., 95-97 percent) was at 253.7 nm. The photon dose rate into 1 L of solution in the reactor system just described was determined by chemical actinometry to be 100.6 μ M photons/

minute (μ E/L-min) when two lamps were used. Hydrogen peroxide was used as the actinometer.

Miniature photolysis system.

For photolysis experiments that required a volume of reactants of less than 50 mL, an additional reactor system was used. It consisted of a graduated cylinder that was 25 mm in diameter and 240 mm in height. The quartz lamp well was inserted into the cylinder and secured with a clamp. Mixing was achieved by using a magnetic stir bar. If required, the contents of the cylinder were sparged with oxygen or nitrogen. The sparge gas was introduced through a 9-in. Pasteur pipette, which had been inserted between the quartz lamp well and the interior wall of the cylinder and which extended to within 2 cm of the liquid surface in the reactor.

Chemicals, Reagents, and Standards

All chemicals were reagent grade or the best grade available and were used without further purification. Deionized water treated by a Barnstead Nanopure[®] purification system (consisting of one pretreatment, one organics removal, and two ion exchange cartridges) was used in all experiments and reagent preparations, except where noted. For analyses of the short-chained organic acids using HPLC and UV detection at 210 nm, reagent grade water was used.

Experimental Methods and Procedures

Analytical Methods

HPLC ordnance screening method.

The ordnance screening analysis used in this laboratory was an adaptation of U.S. Environmental Protection Agency (EPA) Method 8330. It consisted of an isocratic separation using a mobile phase of methanol and water (40:60, v:v) at a flow rate of 1 mL/min. The analytical column was a Supelco LC-18, which was preceded by a C18 guard column. Detection of analytes was accomplished by monitoring UV absorbance at 254 nm.

Ordnance compound method adaptations for kinetic studies.

Kinetic experiments required conditions with a minimum time for each analysis. Consequently, the organic content of the mobile phase was increased to 60 per-

cent with water comprising the remaining 40 percent. These isocratic conditions shortened the time of analysis for DNT from 30 min to 10 min.

Fractionation of RDX and its by-products (separation of nitroso compounds).

A different mobile phase was necessary to ensure baseline resolution of RDX and the three major photolytic by-products. The two mobile phase components, A and B, were introduced at a ratio of 80:20. Component A was degassed, nanopure water and component B was a mixture of equal volumes of methanol and water. Flow was maintained at 1.0 mL/min. Remaining parameters were identical to those used with the ordnance screening method.

Carbonyl analysis by DNPH derivatization.

Carbonyl compounds, formed as treatment products, were determined by conversion of the aldehyde or ketone to the corresponding hydrazone by derivatization with 2,4-dinitrophenylhydrazine (DNPH). This procedure required the addition of acidic DNPH to the aqueous sample, followed by an 18-hr holding time during which the derivatization occurred. Reagents and sample were sparged with nitrogen to prevent side reactions. An equal volume of methanol was subsequently added to the sample to prevent peak splitting, bringing the organic content of the matrix up to a minimum of 50 percent. The HPLC analytical system consisted of a Supelco LC-18 analytical column fitted with a C18 guard column. Separation of the carbonyl components was achieved with an isocratic methanol/water (60/40, V/V) mobile phase and detection was at 360 nm.

Inorganic analytes.

The nitrate (NO_3^-), nitrite (NO_2^-), and ammonium (NH_4^+) analyses were performed on a Dionex 200i/SP ion chromatograph. Dissolved oxygen (DO) was measured in situ by using an Orion Model 820 DO meter manufactured by Orion Research Incorporated, Boston, MA, with automatic atmospheric pressure, temperature, and salinity corrections. The measurement of DO in the CSTR was made on a stream recirculated by a small pump through a cell in which the electrode was sealed.

Surrogate methods.

Solution pH was measured using a Beckman o-21 pH meter with temperature compensation, with a two-point calibration against commercial standard buffers. All solutions were magnetically stirred during pH measurement. Ultraviolet absorbance at 254 nm was measured using an LKB model 4050 UV/VIS spectro-

photometer. Absorbance at this wavelength was of interest primarily because of the effect of competition of the solution components for 254 nm photons during photolytic studies.

Experiments Using Ordnance Compounds – Photolysis

Aqueous solutions of RDX were typically made up the day before an experiment and allowed to stir overnight in a foil covered flask. The solution was transferred to the reactor prior to the experiment and sparged with either oxygen or nitrogen if a certain DO concentration was required. DO measurements were made in situ but discrete samples were required for all remaining analyses. In the small stirred-tank reactor, a syringe was used to aspirate a volume through a 1/8-in. PTFE line, which had been inserted through one of the twin angled joints (24/25 Standard Taper joint) of the glass cover. Experiments in organic solvents were conducted in either a clear, 40 mL vial or a 100 mL graduated cylinder with the RDX solution made immediately prior to use. Samples were removed by aspiration using a Pasteur pipette while a teflon-coated stir bar provided mixing. If the conditions of the experiment required control of the DO, a sparge gas was introduced through a Pasteur pipette. Analyses were performed using the analytical methods described beginning on p 35.

5 Results and Discussion

Product Yield Diagrams

Description

A useful tool in interpreting the experimental data is the calculation of the cumulative yield of a product as the reaction proceeds, defined as:

$$\text{product yield} = \frac{\text{product formed}}{\text{RDX consumed}}$$

where product and RDX are expressed in molar units. Normalizing by-product formation to the amount of RDX consumption can provide information about reaction stoichiometry and mass balance. It also allows easy comparison of experiments, even if the RDX photolysis rates vary slightly from day to day. The product yield was calculated using the experimental data from photolysis experiments, and plotted versus the extent of RDX conversion (i.e., the fraction of RDX consumed [0 to 1]) to give an overall picture of the product behavior during the reaction. All yield diagrams are undefined at zero RDX conversion. However, in principle, if the yield extrapolates to a nonzero value at low RDX conversions, it is implied that either all substances required to produce the product are present initially, or they are produced and react very quickly as the reaction proceeds. Under these conditions, information on stoichiometry or branching ratios of early steps can be obtained. If, on the other hand, the yield increases with conversion and extrapolates back to zero at very low RDX conversions, it implies that a necessary component must accumulate before product formation can occur, and that reaction with the produced intermediate is slower.

Interpretational difficulties for the yield values can be encountered in practice, however, due to problems associated with analytical precision in the early stages of reaction, since the calculated value of RDX consumed (ΔR) can be a small difference between the relatively large initial RDX concentration and the concentration of RDX remaining at small time t . The amount of uncertainty in the value of ΔR can be comparable to or larger than the amount of product formed, and erratic calculated values of the yield can result from a small amount of data scatter early in the experiment. Similarly, an artifact can arise from, for exam-

ple, the inadvertent appearance of a small constant peak in the HPLC or GC chromatogram that is buried under the product peak. Such an artifact can cause a significant apparent increase in the product yield early in the reaction, which would decrease rapidly as the product peak grew. Figure 6 shows a hypothetical example that compares the calculated yield diagrams for a product formed in constant 14 percent yield from the parent compound, with and without an impurity in the product peak, corresponding to 0.5 percent of the parent compound. The artifact causes a very high apparent yield early in the reaction, which drops off rapidly as the amount of product increases and the amount contributed by the impurity decreases in significance. A similar effect could be caused by a nonlinearity or a positive nonzero intercept in the concentration-response curve for the analyte, due to nonideal integration of the analyte peak. Despite these inherent difficulties, if interpreted with care, yield diagrams can provide important information about reaction pathways.

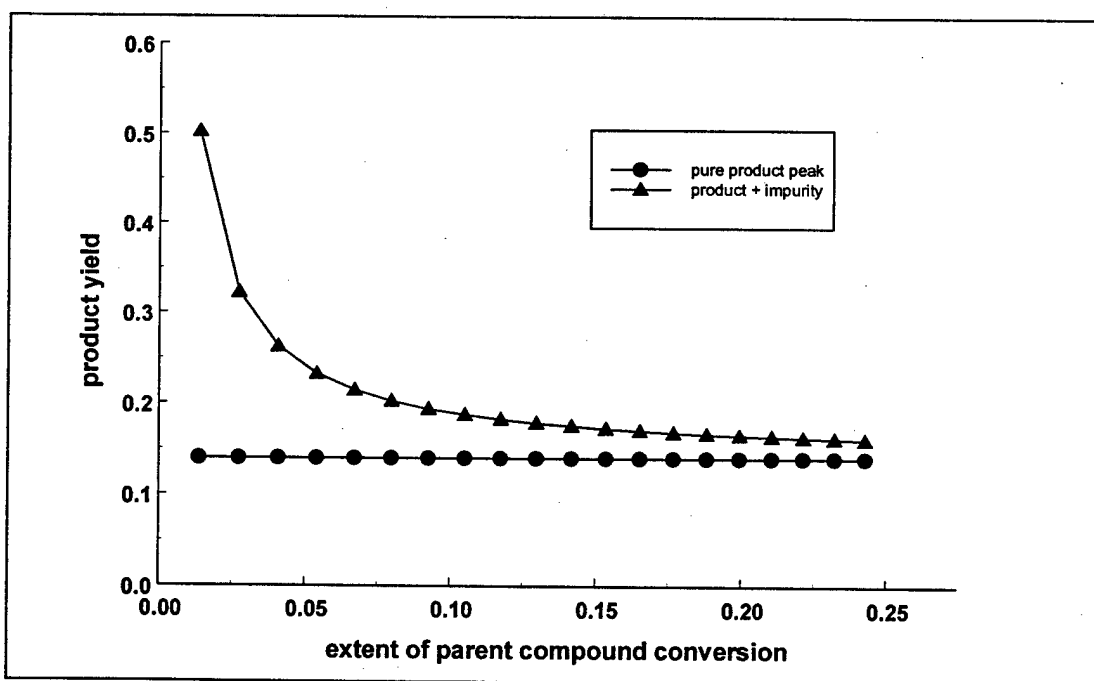


Figure 6. Effect of 0.5% impurity in chromatogram peak on calculated product yield.

MNX Yield Diagrams

MNX yield diagrams for two aqueous RDX photolysis experiments are shown in Figure 7, where a suspiciously high MNX yield is seen in the early stage of conversion for the nitrogen-sparged experiment (solid triangles). The calculated yield for the off-scale point in that experiment was approximately 1. Similar plots for other experiments (not shown) gave very similar curves, except for the early region, where the increase in yield at low extent of conversion was considerably less pronounced. No mechanism could be found that would explain a

burst of MNX production at the beginning of the experiment, but that would then "shut off" after the first 10 to 15 percent of RDX conversion. The inconsistency of the early regions for the two curves, coupled with the similarity of the shape of the data plot at higher extent of conversion, is consistent with the existence of artifacts arising from the precision of measuring low concentrations of MNX, and of subtracting RDX concentrations from $[RDX]_0$ to calculate ΔR at low RDX conversions. Further evidence for this conclusion will be presented during the discussion of numerical modeling.

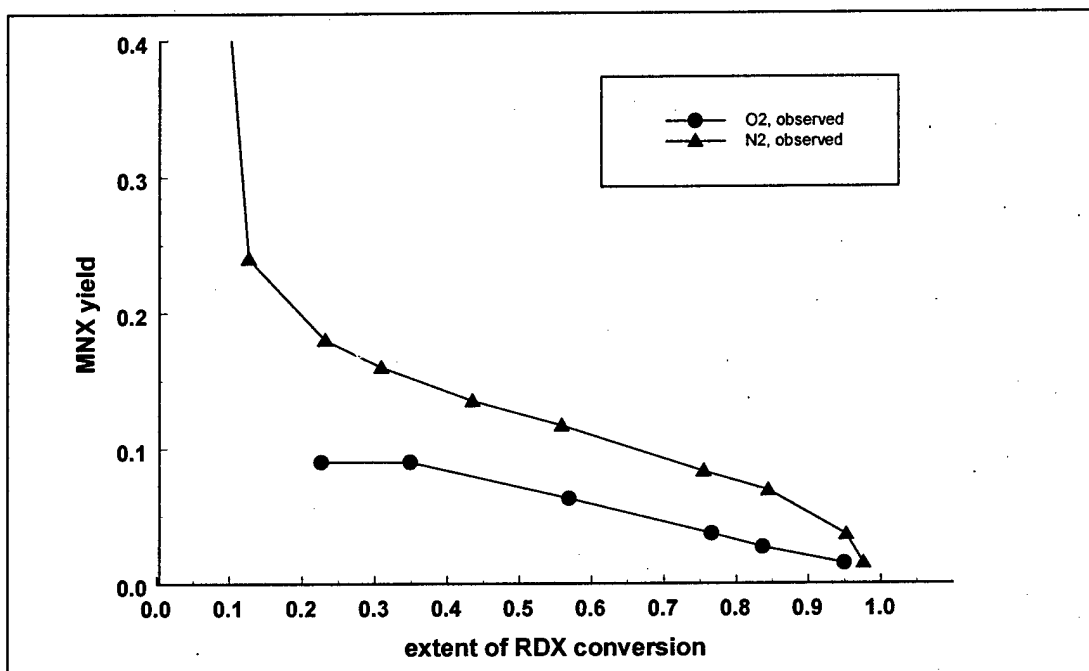


Figure 7. Yield of MNX under oxygenated and deoxygenated (N_2 sparged) conditions.

By-Product Yield Diagrams – Formaldehyde

The yields of formaldehyde for the above experiment are shown in Figure 8. The formaldehyde yield of 2.8-3.0 shown in Figure 8, when added to the carbon present in the nitroso derivatives, accounts for all of the carbon present in the parent compound, with a slight excess. The excess is within the sum of the experimental error for the several measurements that are involved. It is important to note that the analytical method for formaldehyde includes a derivatization step that involves standing overnight in an acidic solution of DNPH (2,4-dinitrophenylhydrazine), so that any by-products that hydrolyze to formaldehyde are also represented in the quantity of formaldehyde reported. Neither RDX nor the nitroso compounds hydrolyze under these conditions, but the unsaturated compounds may be expected to undergo hydrolysis. Furthermore, due to the acid conditions during derivatization, nitrite present in the sample is converted to nitrous acid,

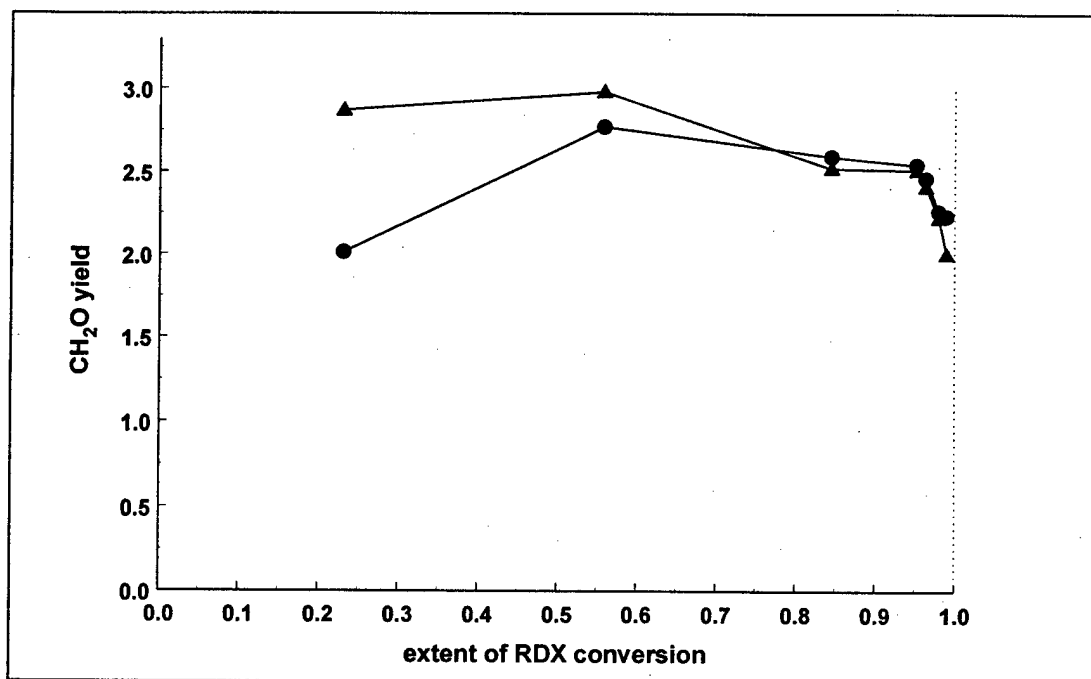
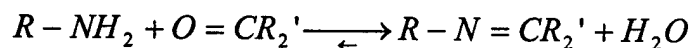


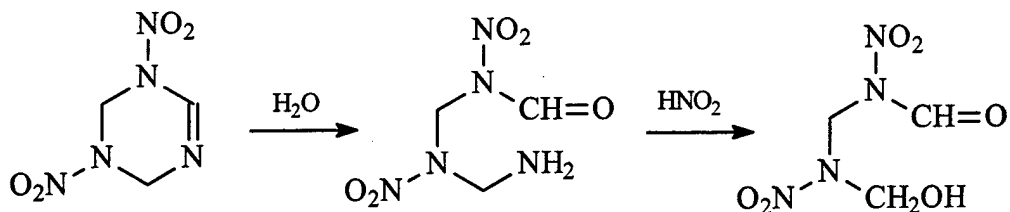
Figure 8. Formaldehyde yield under oxygenated (●) and deoxygenated (▲) conditions.

which can further react with amines and amides (such as substituted ureas) in the reagent solution. Nitrous acid reacts with primary amines to form diazonium salts, which decompose, liberating nitrogen gas and a carbonium ion that can produce various organic products such as alcohols, or undergo carbon-nitrogen (C-N) bond cleavage (Noller 1965). This reaction is sufficiently quantitative that it is the basis for some analytical methods for amines, amino acids, and proteins. Nitrous acid also reacts with ureas and amides (RCONHR') to liberate nitrogen.

It is well known in organic chemistry that amines and carbonyl compounds form addition compounds, called enamines:



It is interesting to note that the unsaturated derivatives such as MUX have this C-N double bond structure, which may account for their ease of hydrolysis (observed at least in the two known cases of MUX and triazine). Hydrolysis of MUX would lead to a primary amine, which would then be susceptible to attack by nitrous acid under the conditions of the formaldehyde analytical method, eliminating N₂ and leaving a carbon-centered functional group such as the alcohol shown below, or C-N bond cleavage.



It is interesting that the product of this reaction is the same as that which is obtained by applying the proposed mechanism of Oxley et al. to RDX (see **Nitramine and Nitrosamine Photolysis/Thermolysis Literature**, Chapter 2). It is possible to hypothesize subsequent degradation steps leading completely to small molecules, particularly for the doubly unsaturated compound DUX, but without positive identification of by-products other than MUX, it is of little value. Isolation and identification of such unstable by-products is difficult at best, and the steps that occur in acidic solution under the conditions of the formaldehyde analysis are not necessarily the predominant ones that occur in neutral solution. Most significant is the implication from the carbon mass balance data provided by the formaldehyde analysis, that the large majority of all by-products, other than the nitroso compounds MNX, DNX, and TNX, are susceptible to hydrolysis and/or nitrous acid attack, implying that they are unsaturated, amines, amides, etc. These reactions take place on a different time scale than do the photolytic and free-radical reactions being studied, and continue long after photolytic treatment stops (i.e., time scale of tens of minutes to hours, rather than milliseconds to minutes).

Importance of Nitrous Acid Reactions in the Formation of MNX During RDX Photolysis

The preceding discussion raises the question of whether nitrous acid reactions play a significant part in formation of MNX. Nitrous acid reacts with secondary amines to produce nitroso compounds, and this reaction has been suggested as a possible pathway. Consistent with this suggestion were the results of Kubose and Hoffsommer (1977), that the nitroso derivatives were only observed upon photolysis of RDX in acidic solution, and then, only at about 1 percent yield. On the other hand, in this study MNX and DNX formations were observed in neutral aqueous solution at yields in the 10 to 15 percent range. Kubose and Hoffsommer used a medium-pressure UV lamp, instead of a low-pressure lamp as used in this study, which may account for some of the differences, due to the difference in spectral output.

To determine if nitrous acid was active in the formation of MNX, RDX was photolyzed in three experiments in aqueous solution at pH values of 3.1, 5.3, and 7.0. The pK_a of nitrous acid is 3.4, so more than half of the nitrite produced would have been in the form of nitrous acid in the pH 3.1 experiment. The MNX yields for those three experiments are shown in Figure 9, where it is seen that pH had little effect on the MNX yield, with the greatest yield being obtained at pH 7.0, rather than at lower pH. Thus, it is concluded that nitrous acid does not participate in the formation of MNX during photolysis of aqueous RDX solutions.

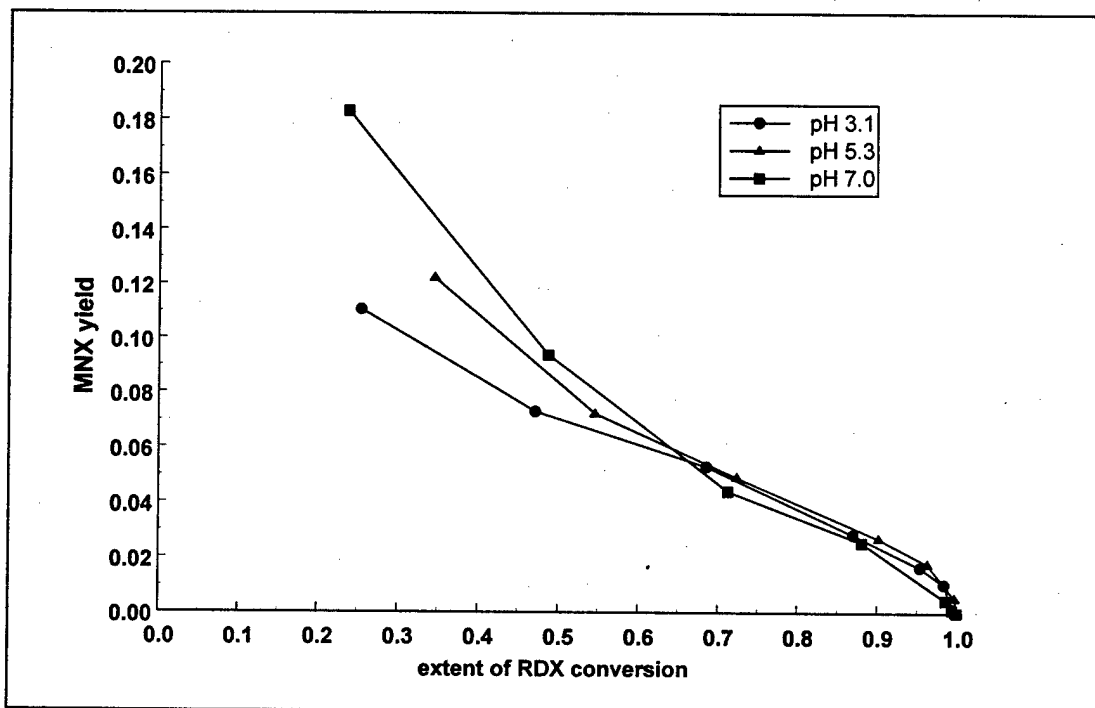


Figure 9. MNX yield as a function of pH.

Inorganic Nitrogen Compound Formation During RDX Photolysis

During the above experiments, measurements were also taken for several inorganic nitrogen compounds that occurred as by-products during RDX photolysis. Yield diagrams are shown for nitrite, nitrate, and ammonium ions during RDX photolysis in an oxygen-sparged (Figure 10) and nitrogen-sparged (Figure 11) aqueous solution. In the oxygenated solution (Figure 10), the yield of nitrite appears to build gradually, while in the deoxygenated solution (Figure 11), after low production initially, nitrite appears to build quickly between 20 and 50 percent RDX conversion. In both solutions, a maximum yield of about 2 was reached (slightly higher in oxygenated solution). A final nitrate yield of about 1 was obtained in the oxygenated solution, compared to about 0.5 in deoxygenated solution. In both experiments, a maximum ammonium yield of about 0.75 was reached. Thus, a maximum nitrogen mass balance of about 3.75 out of 6 was

attained. Interpretation of the nitrogen mass balance data is complicated by the fact that by-products on the MUX side of the degradation mechanism can hydrolyze appreciably before they are analyzed for the inorganic nitrogen compounds under the conditions used. Therefore, some fraction of the yields of these compounds may have been formed in the reaction vial, rather than in the reactor during photolysis.

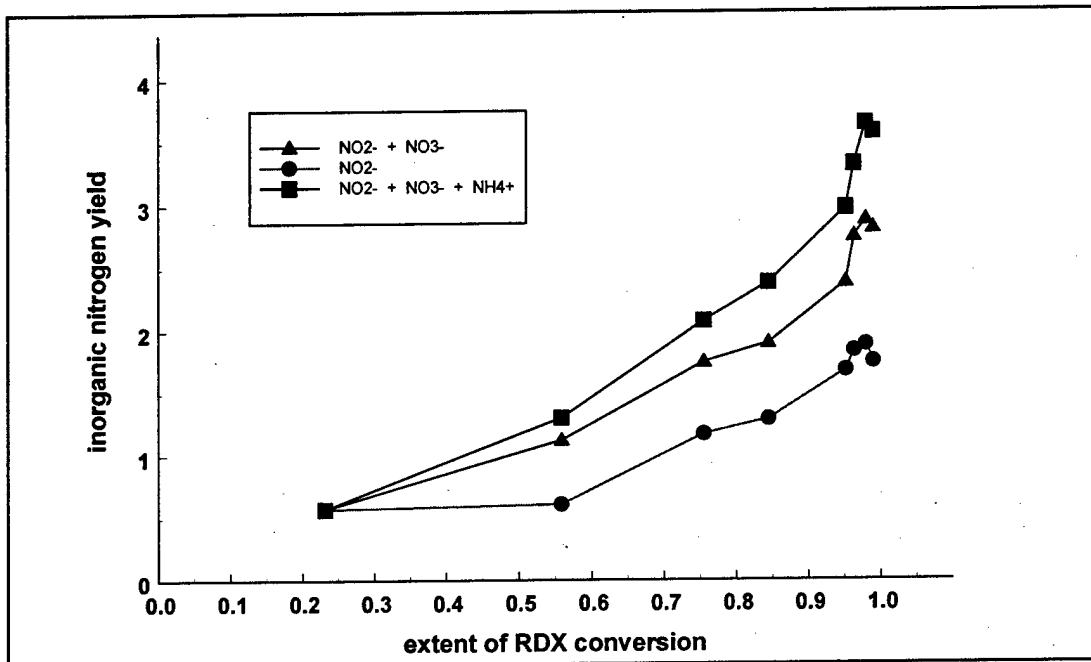


Figure 10. Inorganic nitrogen yields under oxygenated conditions.

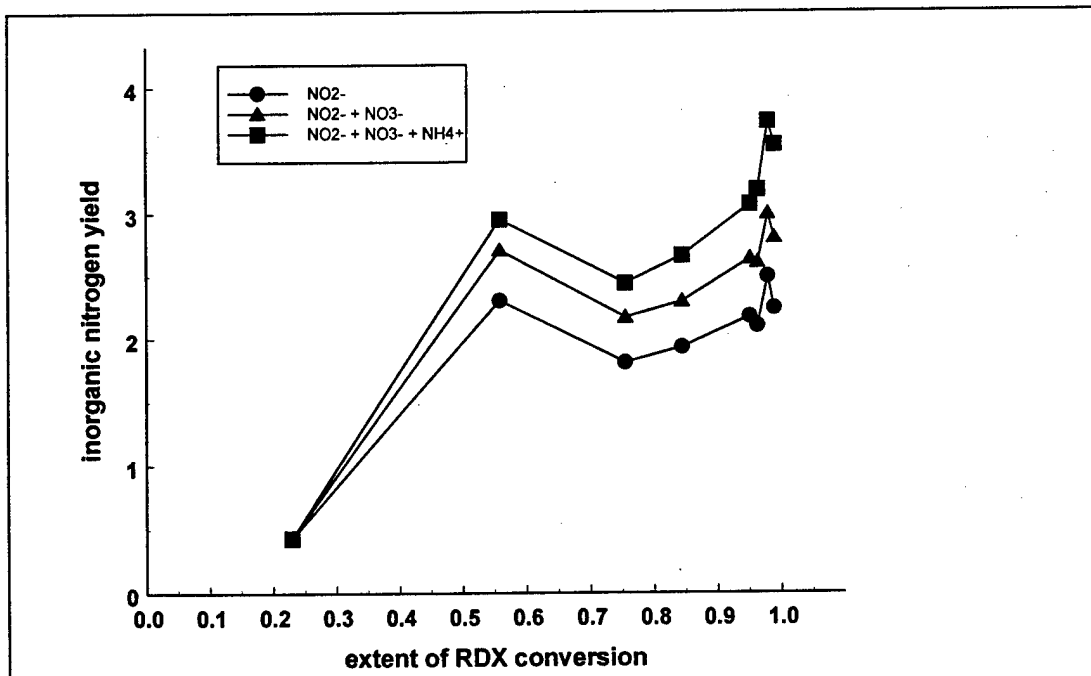


Figure 11. Inorganic nitrogen yields under deoxygenated conditions.

There are four primary channels by which nitrite can form in this system: (1) through hydrolytic disproportionation of NO_2 , which also produces nitrate in an equal amount, (2) as a by-product of the reaction between N_2O_3 and a secondary amine such as A, (3) through hydrolysis of unstable products such as the unsaturated product MUX, and (4) by direct elimination of HNO_2 from a nitramine such as RDX, if this elimination occurs. Nitrate ion can arise primarily from two sources. The first is the disproportionation of NO_2 , as mentioned earlier. The second is as a by-product of the reaction of N_2O_4 with a secondary amine in the reaction that forms a nitroso compound:



These reactions will be examined in greater detail in the discussion of the modeling results.

In many literature accounts, nitrogen gas and N_2O have been found as products. If nitrogen or N_2O were formed in the present study, they would have gone undetected, since no measurements were made on the gas phase. In addition, a different sparge gas such as argon would have been required, rather than nitrogen. Formation of one molecule of nitrogen or N_2O per RDX molecule consumed would bring the observed mass balance up to 5.75 out of 6, which is within experimental error of mass balance closure. The mechanism by which nitrous acid reacts with primary amines to liberate nitrogen is through the formation of N_2O_3 (Noller 1965). For the present system, nitrous acid reactions have been shown to be unimportant, but N_2O_3 is produced by a different pathway, which is the reaction between NO and NO_2 . It is interesting to note that, if the hypothesized hydrolysis step that was illustrated in the previous section for MUX were to occur, N_2O_3 or N_2O_4 would rapidly react with the resulting primary amine, liberating one molecule of nitrogen gas and producing nitrite or nitrate, respectively, as a by-product.

Investigations of the MUX Reaction Channel

In earlier work (Peyton and LeFavre, unpublished data), the rate of hydrolysis of a transient product thought to be MUX was determined, for comparison with information from the literature.

Another determination was made of the rate constant for the hydrolysis of the compound assigned to the structure of MUX. RDX was photolyzed in water for 10 seconds to give 36 percent RDX removal, then a sample was quickly placed in

an autosampler vial and repetitive injections made into the HPLC. Figure 12 shows the disappearance curve of MUX in that experiment. The pseudo-first-order rate constant was obtained as the slope of a plot of the natural logarithm of [MUX] vs. time (not shown). The value was found to be $3.3 \times 10^{-4} \text{ sec}^{-1}$ at pH 7.08, in reasonable agreement with previous values of $1.1 \times 10^{-4} \text{ sec}^{-1}$ (50:50 acetonitrile:water) and the values of 0.76×10^{-4} and 2.8×10^{-4} at pH 7.28 and 7.89, respectively, reported by Hoffsommer, Kubose, and Glover (1977).

Another experiment was performed to verify that this was indeed a hydrolysis reaction. RDX was photolyzed for 10 seconds to give 34 percent conversion in dry acetonitrile and a sample of the acetonitrile placed in an HPLC autosampler vial for repeated injections without prior dilution with water. The peak area of the product increased by a factor of 2 over the first 5 h, then dropped off sharply, and decreased by half the amount of the previous increase over the next 5 h. This acetonitrile solution was allowed to stand overnight, then analyzed the next morning, and the product peak in the HPLC chromatogram was found to have approximately the same area as on the previous evening. This solution was then diluted with an equal volume of water to initiate hydrolysis, and again subjected to repetitive injections. A rapid decrease in peak area was noted, with a half-life of about an hour, for which the pseudo-first-order rate constant for the transient disappearance was found to be $2.9 \times 10^{-4} \text{ s}^{-1}$.

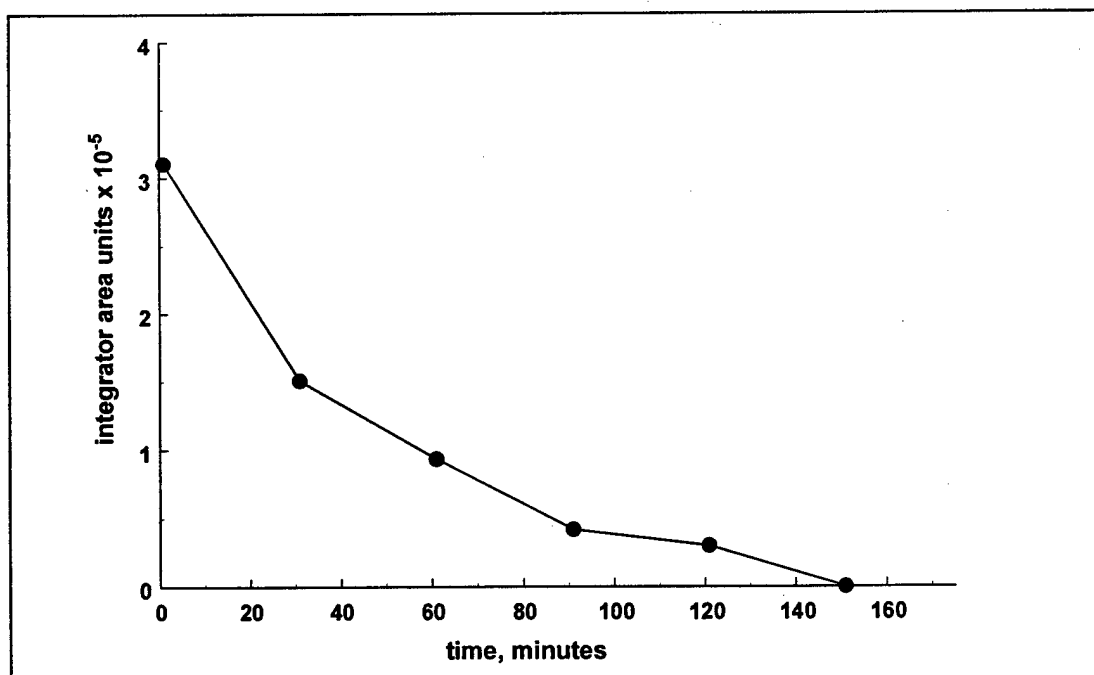


Figure 12. Hydrolysis rate of MUX.

A third solution of RDX in acetonitrile was photolyzed in the same manner (35 percent in 10 sec). Instead of being allowed to stand, however, it was immediately diluted with water and repetitively injected into the HPLC. The peak area first increased somewhat, then decreased with a pseudo-first-order rate constant of $2.6 \times 10^{-4} \text{ s}^{-1}$. It appears that the increase seen in the previous solution represented the "growing in" of another compound, which then underwent conversion to still another species. Another possibility is that the first compound continued to grow in competition with hydrolysis or another reaction, until water or other reactant was consumed. Regardless of whether the final mixture in acetonitrile represented one compound or several, the hydrolysis went to completion upon addition of water with a rate constant that is within experimental error of the other values quoted above for the compound assigned the structure of MUX.

On the basis of the above experiments, it is concluded that the compound produced during RDX photolysis in acetonitrile is the same as that produced upon photolysis in water, and that the reaction that it undergoes in aqueous solution is indeed a hydrolysis reaction. Based on the similarity of hydrolysis rate constants between this compound and that observed by Hoffsommer, Kubose, and Glover (1977), it is concluded that the by-product obtained in this study is the same as observed by those authors upon basic hydrolysis of RDX. Based on the fact that their product was obtained by basic hydrolysis of RDX, and its identification is based upon the mass spectrum obtained by those authors, we agree with their conclusion that this compound is the first unsaturated derivative of RDX, referred to as MUX in this study. It can also be concluded that samples will change appreciably within a short time, so that analyses performed on aqueous solutions as soon as the next day can be expected to reflect the products of hydrolysis, not those intermediates that were present at the time of sampling. This complicates the interpretation of analytical results for formaldehyde and inorganic nitrogen compounds reported earlier.

Kinetic Modeling of RDX Photolysis

Solution of Kinetic Equations

Simplification of the rate equations through the use of the steady-state assumption was carried out in an attempt to arrive at versions of the equations that would be useful in data interpretation. In particular, the limit of the ratio of the rate equations for MNX and RDX, as the extent of conversion approached zero, should extrapolate to the initial MNX yield value at low RDX conversion. However, the ratio of the MNX and RDX equations derived from the simplification of the kinetic equations gave an expression that depended primarily on several

species concentrations and rate constants that were not known, making it of little value as an interpretative tool. It was therefore necessary to numerically integrate the rate equations and obtain values of some parameters by fitting, as described below.

Numerical Integration of the Rate Equations and Fitting of Rate Constants

The reactions in Table 1 were used to construct the rate equations, as described earlier. The equations were numerically integrated out to a final time that corresponded to 90+ percent RDX removal. Since the calculations predict the species concentrations throughout the reaction, rates of individual processes can be compared to determine primary and secondary pathways within the mechanism. Because this model does not explicitly include DNX and TNX, the results at later times are questionable, compared to results earlier in the reaction, when MNX is the primary product.

Table 1 lists the values of the rate constants used in the final simulation. The value of k_1 was obtained experimentally, as the first-order disappearance rate constant for RDX. The value for k_{sc} was estimated as one order of magnitude lower than the measured value for RDX + hydroxyethyl radical by analogy with the findings of Jagannadham and Steenken (1984), who reported that hydroxymethyl radical rate constants for reaction with nitroaromatic compounds were about an order of magnitude smaller than those for hydroxyethyl radical. Variation of this rate constant showed the calculation to be insensitive to even a two orders-of-magnitude change. The same calculations showed that the reductive reaction $RDX+S \rightarrow Q$ is unimportant in this system, because the rate of MNX production by this channel is several orders of magnitude slower than that through the amine nitrosation channel.

The values of the rate constants for $R+R$ and $R+NO$ were taken to be 1×10^9 , based on typical values for radical-radical reactions, including aminyl radicals. The value for $R+Donor$ was set slightly higher than the known value for piperidyl radical +methanol. Formaldehyde was considered to be the H-atom donor in this calculation, but it is possible that other byproducts participate, as well. The value for $R+O_2$ was started at the lower end of the range estimated from the literature for aminyl radicals (1×10^4 to $1 \times 10^6 \text{ M}^{-1}\text{s}^{-1}$, see discussion in an earlier section), and varied as a parameter, giving the final value 8×10^3 .

No value could be found from which to estimate the rate constant for rearrangement of the aminyl radical to a carbon-centered radical. As far as the pathway diagram is concerned, this reaction has the same effect as reaction of R with

oxygen: R is diverted from the MNX subsystem (i.e., an "escape" reaction) and the resulting product is MUX. Therefore, for purposes of modeling the MNX subsystem, the ratio of $k_{RX}[O_2]$ and k_{rt} determines the oxygen dependence of the escape reaction. Satisfactory results were obtained setting k_{rt} to 1.0 s^{-1} , compared to $k_{RX}[O_2] = 8 \times 10^3 (1 \times 10^{-5} \text{ to } 1 \times 10^{-3}) = (0.08 \text{ to } 8.)$.

Relative values for the rate constants for reaction of amine A with N_2O_3 and N_2O_4 were determined by setting $k_{TA} = k_{EA}/2$, in accordance with the observations of Challis and Kyrtopolis (1978; 1979). It was found necessary to increase k_{TA} slightly (5.0×10^8 in the present work) over the range of literature values of (7.5×10^7 to 3.1×10^8) found by Casado et al. (1983), for various aliphatic amines. Values for the reactions between $NO_2 + NO_2$, $NO + NO_2$, $NO_2 + NO_2 + H_2O$, and $NO + O_2$ were taken directly from the literature. Rate constant values for the reverse reactions $N_2O_3 \rightarrow NO + NO_2$ and $N_2O_4 \rightarrow 2 NO_2$ were calculated from the equilibrium constant at $25 \text{ }^\circ\text{C}$ to be 8.0×10^4 and 7.0×10^3 , respectively. It was found necessary to decrease the latter value to 1×10^3 to fit the present data.

The value of the rate constant for the photolysis of MNX to produce NO and NO_2 were set initially to 1×10^{-3} , based on the value for the similar photolysis, k_1 . The value for k_p was later adjusted to 1.5×10^{-3} to obtain a better fit at higher RDX conversions, but it must be kept in mind that this incomplete model does not include the effects of DNX and TNX. Therefore, the model cannot be expected to fit the latter part of the yield curve as well as it should fit the earlier part.

Results of Data Fitting

The fit of the kinetic model to the data from the oxygen- and nitrogen-sparged experiments discussed above is shown in Figure 13. The solid symbols represent experimental data, while the open symbols are the predictions calculated from the model. The calculated and experimental results differ considerably for the first three points shown in Figure 13. The error bars on points from the deoxygenated experiment represent the uncertainty introduced by the relative standard deviation of the measured MNX and RDX concentrations, and the calculated results fall inside these error boundaries except for the first two points. The unrealistically high values of the yield for points at low values of RDX conversion were discussed in connection with Figure 6 and 7, and are thought to be analytical artifacts. Therefore, the model was fit to only the central portion of the data corresponding to RDX conversions of 0.3 to 0.7.

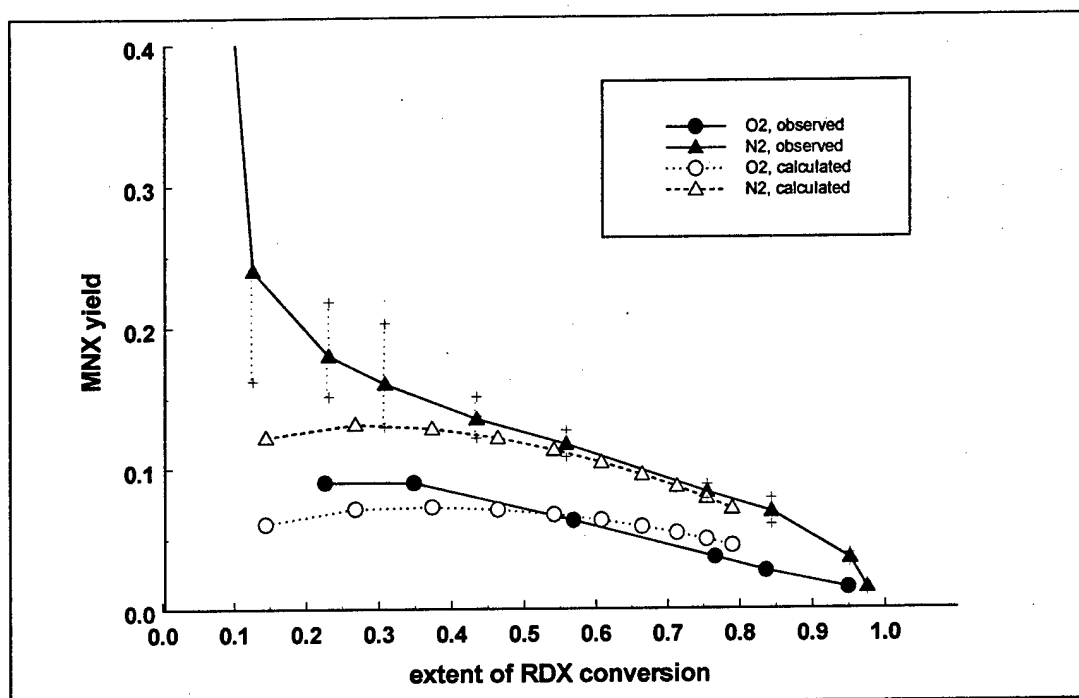


Figure 13. Comparison of model predictions to actual results for oxygenated (O₂) and deoxygenated (N₂) conditions.

Several observations can be made from the numerical values of the species concentrations that were calculated by the rate equation integration:

1. The parameter f_1 was intended to represent the fraction of RDX that decomposed through the pathway to NO₂ and aminyl radical, compared to other unspecified pathways such as direct elimination of HNO₂. It was found necessary to set $f_1=1$ to produce sufficient MNX to reproduce the experimental data. This is not in conflict with other investigators' observations, since MUX is produced by other pathways in the proposed mechanism. Thus, the proposed mechanism, if verified, will unify the MNX and MUX channels into one branch coming from a single primary photochemical step.
2. For the rate constants used in the calculation, the effect of NO formation was found to be negligible (i.e., neither reaction with oxygen to produce NO₂ nor reaction with NO₂ to produce N₂O₃ was found to be significant). This was true, in part, because the back reaction of N₂O₄ was sufficiently slow so the primary MNX-forming channel was N₂O₄+A. If the back-reaction rate for N₂O₃ had also been lowered from the literature value somewhat, that pathway might have become very slightly significant. However, since the inorganic nitrogen by-products were not being modeled at this point, the effect on the result of this calculation would be insignificant.

3. About 18 percent of the photolyzed RDX was transformed to MNX in the nitrogen-sparged experiment, not all of which was present at any give time, due to further photolysis. The maximum present at one time was 13 percent at the 27 percent RDX conversion point. Since the transformation creates nitrate, between 18 percent and 3×18 percent = 54 percent yield of nitrate would be expected due to this source, depending on the efficiency of DUX and TUX generation.
4. In the deoxygenated experiment, 45 percent of the RDX reacted produced the amine A, while in the oxygen experiment, only 13 percent made it that far into the MNX channel. This difference is due almost entirely to competition for aminyl radical R by oxygen, sending reaction flux through the MUX channel, rather than the MNX channel. The difference between flux to A and all the way through to MNX is caused by the limited availability of the nitrosating agent N_2O_4 . In both the oxygenated and deoxygenated experiments, more A was produced by disproportionation of R than by reaction of R with Donor (formaldehyde).
5. Of all the NO_2 being formed at the 37 percent RDX conversion point, 23 percent and 50 percent hydrolyzed (to nitrate and nitrate) in the N_2 and O_2 sparged experiments, respectively, while the other 77 percent and 50 percent, respectively, reacted to form N_2O_4 . Therefore, the higher MNX production in the deoxygenated system was due to greater availability of the nitrosating agent. These hydrolytic yields would contribute half that amount to the nitrate yield (12 percent and 25 percent, respectively), with the balance of the nitrate yield due to formation during nitrosation. The percentage yields listed above change with the extent of RDX removal.

6 Conclusions

1. Modeling of the MNX subsystem provided insight into the primary pathway in MNX formation during RDX photolysis, and allowed some terms in the rate equation to be discarded.
2. The product yield per RDX consumed is a useful quantity for understanding RDX photolysis pathways. This quantity can be used in conjunction with reaction rates predicted by the model to estimate flux through various channels.
3. The main pathway in RDX photolysis to produce MNX is loss of NO_2 , followed by disproportionation or reaction of the aminyl radical thus formed with an H-atom donor to produce the corresponding amine. The amine is then nitrosated by the N_2O_4 formed by dimerization of NO_2 . Reducing-radical attack upon RDX to cause direct reduction to the nitroso compound does not appear to be important in the aqueous system.
4. Although a considerable fraction of photolyzed RDX appears to go through an alternate reaction channel, which appears to involve formation of the unsaturated product MUX, there is a single primary photochemical step, with branching occurring at the aminyl radical reaction stage.
5. Although hydrolysis of NO_2 is an important reaction, it is by no means dominant, allowing nitrosation of the amine by N_2O_4 .
6. The portion of the reaction that goes through the MUX side of the mechanism appears to produce unsaturated compounds that are easily hydrolyzable. An early product thought to be MUX hydrolyzed with a rate constant of $3 \times 10^{-4} \text{ s}^{-1}$ (half-life of about 40 min), making identification of these transient products difficult.
7. The reductive reaction carried out by donor radicals appears to be unimportant in this system.

References

- Asmus, K.D., H. Mockel, and A. Henglein, *J. Phys. Chem.* 77(1973)1218-1221, and references therein.
- Aurich, H.G., "Nitroxides," in Breuer, E., H.G. Aurich, and A. Nielsen, *Nitrones, Nitronates, and Nitroxides* (John Wiley & Sons, 1989), p 320.
- Awad, H.H., and D.M. Stanbury, *Int. J. Chem. Kinet.* 25(5)(1993)375-81.
- Botcher, T.R., and C.A. Wight, "Explosive Thermal Decomposition Mechanism of RDX," *J. Phys. Chem.* 98(1994)5441-5444.
- Bowman, D.F., T. Gillan, and K.U. Ingold, "Kinetic Applications of Electron Par-amagnetic Resonance Spectroscopy. III. Self-Reactions of Dialkyl Nitroxide Radicals," *J. Am. Chem. Soc.* 93(1971)6555-6561.
- Casado, J., M. Mosquera, L.C. Paz, M.F.R. Proeto, and J.V. Tato, "Nitrite Ion as a Nitro-sating Agent. Nitrosation of Morpholine and Diethyl Amine in the Presence of Formal-dehyde," *J. Chem. Soc., Perkin Trans. II* (1984)1963-66.
- Casado, J., A. Castro, J.R. Leis, M.A. L. Quintela, and M. Mosquera, "Kinetic Studies on the Formation of N-Nitroso Compounds VI. The Reactivity of N₂O₃ as a Nitrosating Agent," *Monatshefte fur Chemie*, 114(1983)639-646.
- Challis, B.C., and S.A. Kyrtopoulos, *J. Chem. Soc., Perkin II* (1978)1296-1302.
- Challis, B.C., and S.A. Kyrtopoulos, *J. Chem. Soc., Perkin I* (1979)299-304.
- Chow, Y.L., "Nitrosamine Photochemistry: Reactions of Aminium Radicals," *Accts. Chem. Res.*, 6, (1973), 354-360.
- Chow, Y.L., H. Richard, R.W. Snyder, and R.W. Lockhart, "Generation of Aminyl and Aminium Radicals by Photolysis of N-nitrodialkylamines in Solution," *Can. J. Chem.* 57, (1979), 2936-43.
- Dean, J.A., "Handbook of Organic Chemistry" (McGraw-Hill, New York, 1987), p 324.
- Flournoy, J.M., "Thermal Decomposition of Gaseous Dimethylnitramine," *J. Chem. Phys.* 36(1962)1106.
- Geiger, G., and J.R. Huber, "Photolysis of Dimethylnitrosamine in the Gas Phase," *Helv. Chim. Acta*, 64(1981)989-995.
- Graetzel, M., A. Henglein, J. Lilie, and G. Beck, "Elementarprozesse der Oxydation und Reduktion des Nitritions," *Ber. Bunsenges. Phys. Chem.*, 73(1969)646-53.

- Graetzel, M., S. Taniguchi, and A. Henglein, "Pulsradiolytische Untersuchung der NO-Oxydation und des Gleichgewichts $\text{N}_2\text{O}_3 \leftrightarrow \text{NO} + \text{NO}_2$ in waessriger Loesung," *Ber. Bunsenges. Phys. Chem.*, 74(1970)488-492.
- Hawari, J., L. Paquet, E. Khou, A. Halasz, and B. Zilber, "Enhanced Recovery of the Explosive Hexahydro-1,3,5-Trinitro-1,3,5-Triazine (RDX) from Soil," *Chemosphere* 32(1996)1929-1936.
- Ho, T.-I., and Y. L. Chow, "Photochemistry of Nitro and Nitroso Compounds" in *Chemistry of the Functional Groups, Supplement F, The Chemistry of Amino, Nitroso, and Nitro Compounds and their Derivatives, Part 1*, Saul Patai, ed (John Wiley & Sons, New York, 1982).
- Hoffsommer, J.C., and D.J. Glover, "Thermal Decomposition of 1,3,5-Trinitro-1,3,5-triazacyclohexane (RDX): Kinetics of Nitroso Intermediates Formation," *Combustion and Flame*, 59(1985) 303-310.
- Hoffsommer, J.C., D.A. Kubose, and D.J. Glover, "Kinetic Isotope Effects and Intermediate Formation for the Aqueous Alkaline Homogeneous Hydrolysis of 1,3,5-Triaza-1,3,5-trinitrocyclohexane (RDX)," *J. Chem. Phys.*, 81(1977)380-85.
- Hughes, M.N., "Hyponitrites," *Quarterly Reviews, Chem. Soc. of London*, 22(1968)1-17.
- Ingold, K.U., and B.P. Roberts, "Radical Reaction Rates in Liquids," in *Landolt-Börnstein Numerical Data and Functional Relationships in Science and Technology, New Series, Group II Atomic and Molecular Physics, Volume 13, Subvolume c* (1983).
- Jagannadham, V., and S. Steenken, "One-Electron Reduction of Nitrobenzenes by alpha-Hydroxyalkyl Radicals via Addition/Elimination," *J. Am. Chem. Soc.*, 106(1984)6542-6551.
- Kubose, D.A., and J.C. Hoffsommer, "Photolysis of RDX in Aqueous Solution, Initial Studies," Naval Surface Warfare Center (NSWC)/WOL TR-77-20 (February 1977).
- Neta, P., R.E. Huie, and A.B. Ross, "Rate Constants for Reactions of Inorganic Radicals in Aqueous Solution," *J. Phys. Chem. Ref. Data.*, 17(1988)1027-1284.
- Noller, C.R., *Chemistry of Organic Compounds*, 3rd ed. (W.B. Saunders Company, Philadelphia, 1965), p 261.
- Oxley, J.C., A.B. Kooh, R. Szekeres, and W. Zheng (1994), "Mechanism of Nitramine Thermolysis," *J. Phys. Chem.*, 98(1994)7004-7008.
- Oxley, J.C., M. Hiskey, D. Naud, and R. Szerkes, "Thermal Decomposition of Nitramines: Dimethylnitramine, Diisopropylnitramine, and N-Nitropiperidine," *J. Phys. Chem.* 96(1992)2505-2509.
- Peyton, G.R., M.H. LeFaivre, Oliver J. Bell, and O. Smith, "Advanced Oxidation Treatability Study for Low-Level Ordnance Compounds in Ground Water", Final Batch Testing Report to U.S. Navy, Naval Civil Engineering Laboratory, General Services Administration, Task Number POC171028, April 1992.

- Peyton, G.R., O.J. Bell, E. Girin, and M.H. LeFaivre, "Reductive Destruction of Water Contaminants during Treatment with Hydroxyl Radical Processes," *Environ. Sci. Technol.*, 29(1995) 1710-1712.
- Roberts, J.R., and K.U. Ingold, "Kinetic Applications of Electron Paramagnetic Resonance Spectroscopy. X. Reactions of Some Alkylamino Radicals in Solution," *J. Am. Chem. Soc.*, 95(1973) 3228-3235
- Schuchmann, M.N., and C. von Sonntag, "Heteroatom Peroxy Radicals," in *Peroxy Radicals*, Z.B. Alfassi, ed (John Wiley & Sons, 1997), p 439.
- Smolin, E.M., and L. Rapoport, *s-Triazines and Derivatives* (Interscience Publishers, Inc., New York, 1959), p 12.
- Suryanarayana, K., and S. Bulusu, "Photolysis of Solid Dimethylnitramine: Nitrogen-15 Study and Evidence for Nitrosamine Rearrangement," *J. Phys. Chem.*, 76(1972)496-500.
- von Sonntag, C., and H.-P. Schuchmann, "Peroxy Radicals in Aqueous Solution," in *Peroxy Radicals*, edited by Z.B. Alfassi (John Wiley & Sons, New York, 1997).
- Wagner, B.D., G. Ruel, and Janusz Luszyk, "Absolute Kinetics of Aminium Radical Reactions with Olefins in Acetonitrile Solution," *J. Am. Chem. Soc.*, 118(1966)13-19.

CERL Distribution

Chief of Engineers

ATTN: CEHEC-IM-LH (2)
ATTN: HECSA Mailroom (2)
ATTN: CECC-R
ATTN: CERD-L
ATTN: CERD-M

Industrial Operations Command

ATTN: AMSIO-EQC

US Army Materiel Command (AMC)

Alexandria, VA 22333-0001
ATTN: AMCEN-F

Installations:

Rock Island, IL 61299-7190
ATTN: AMXEN-C
Radford Army Ammunition Plant
ATTN: SMCRA-EN 24141
Aberdeen Proving Ground
ATTN: STEAP-FE 21005
Rock Island Arsenal 61299
ATTN: SMCRI-FW
Harry Diamond Lab
ATTN: Library 20783
Picatinny Arsenal 07806
ATTN: AMSTA-AR-IMC

US Army Materials Tech Lab

ATTN: SLCMT-DPW 02172

US Army Environmental Center

ATTN: SFIM-AEC-NR 21010
ATTN: SFIM-AEC-CR 64152
ATTN: SFIM-AEC-SR 30335-6801
ATTN: AFIM-AEC-WR 80022-2108

Defense Tech Info Center 22304

ATTN: DTIC-O (2)

22
8/99

REPORT DOCUMENTATION PAGE

Form Approved
OMB No. 0704-0188

Public reporting burden for this collection of information is estimated to average 1 hour per response, including the time for reviewing instructions, searching existing data sources, gathering and maintaining the data needed, and completing and reviewing the collection of information. Send comments regarding this burden estimate or any other aspect of this collection of information, including suggestions for reducing this burden, to Washington Headquarters Services, Directorate for Information Operations and Reports, 1215 Jefferson Davis Highway, Suite 1204, Arlington, VA 22202-4302, and to the Office of Management and Budget, Paperwork Reduction Project (0704-0188), Washington, DC 20503.

1. AGENCY USE ONLY (Leave Blank)		2. REPORT DATE November 1999	3. REPORT TYPE AND DATES COVERED Final	
4. TITLE AND SUBTITLE Verification of RDX Photolysis Mechanism			5. FUNDING NUMBERS 61102 BT25 J99	
6. AUTHOR(S) Gary R. Peyton, Mary H. LeFaivre, and Stephen W. Maloney				
7. PERFORMING ORGANIZATION NAME(S) AND ADDRESS(ES) U.S. Army Construction Engineering Research Laboratory (CERL) P.O. Box 9005 Champaign, IL 61826-9005			8. PERFORMING ORGANIZATION REPORT NUMBER TR 99/93	
9. SPONSORING / MONITORING AGENCY NAME(S) AND ADDRESS(ES) Headquarters, Industrial Operations Command ATTN: AMSIO-EQC Bldg #390 Rock Island, IL 61299-6000			10. SPONSORING / MONITORING AGENCY REPORT NUMBER	
9. SUPPLEMENTARY NOTES Copies are available from the National Technical Information Service, 5385 Port Royal Road, Springfield, VA 22161				
12a. DISTRIBUTION / AVAILABILITY STATEMENT Approved for public release; distribution is unlimited.			12b. DISTRIBUTION CODE	
13. ABSTRACT (Maximum 200 words) Nitro-aromatics 2,4,6-trinitrotoluene (TNT) and hexahydro-1,3,5-trinitro-triazine (RDX) are the major constituents of wastewaters discharged from munitions load, assembly, and pack operations at Department of Defense (DOD) facilities. TNT and RDX enter wastestreams during munitions loading and demilitarization. This study focused on a treatment method for RDX. Prior work has shown that simple photolysis using ultraviolet light (UV) is sufficient to convert RDX in contaminated water to small non-nitrated organic by-products such as formaldehyde and formic acid, as well as the inorganic ions nitrate and nitrite. This implies that UV photolysis might provide a satisfactory and economical treatment system for RDX in water. The objectives of this project were to postulate a mechanism for RDX photolysis based on information from the literature and data obtained during this study, develop the corresponding kinetic model, and compare projections with results from laboratory photolysis and thermolysis experiments, for the purpose of verifying the model's appropriateness, finding the primary mechanistic steps in RDX photolysis and determining whether the reductive pathway contributes significantly to RDX degradation. Modeling results indicated that, of the possible pathways given in the literature, the primary photolysis pathway to the nitroso derivative in aqueous solution was scission of the N-N bond, eliminating the NO ₂ group.				
14. SUBJECT TERMS hazardous waste minimization munitions waste disposal hexahydro-1,3,5-trinitro-triazine (RDX) photolysis wastewater treatment			15. NUMBER OF PAGES 58	
			16. PRICE CODE	
17. SECURITY CLASSIFICATION OF REPORT Unclassified	18. SECURITY CLASSIFICATION OF THIS PAGE Unclassified	19. SECURITY CLASSIFICATION OF ABSTRACT Unclassified	20. LIMITATION OF ABSTRACT SAR	